

Integrated uppermost Campanian–Maastrichtian calcareous nannofossil and foraminiferal biostratigraphic zonation of the northwestern margin of Australia

R. W. HOWE^{1,2}, R. J. CAMPBELL¹ & J. P. REXILIUS³

¹School of Earth & Geographical Sciences, The University of Western Australia, 35 Stirling Highway, Crawley, WA 6009, Australia (e-mail: rhowe@geol.uwa.edu.au, rcampbel@geol.uwa.edu.au)

²Current address: Energy & Geoscience Institute, The University of Utah, 423 Wakara Way, Suite 300, Salt Lake City, UT 84108, USA (e-mail: rhowe@egi.utah.edu)

³International Stratigraphic Consultants Pty Ltd, 73 Rule St., North Fremantle, WA 6159, Australia (e-mail: jrex@iscbiostrat.com)

ABSTRACT – During the latest Campanian–Maastrichtian the northwestern Australian margin was situated between the cool-water Austral Province to the south and the warm-water Tethyan Province to the north. The transitional nature of calcareous microfossil assemblages on the margin makes application of Tethyan biostratigraphic zonation schemes awkward, as many marker-species are missing or have different ranges. This study presents an integrated uppermost Campanian–Maastrichtian calcareous microfossil zonation based on two Ocean Drilling Program (ODP) holes on the Exmouth Plateau and eight petroleum exploration wells from the Vulcan Sub-basin. The zonation is refined and revised from the previously unpublished KCN (nannofossils), KPF (planktonic foraminifera), KBF (benthonic foraminifera) and KCCM (composite nannofossil and planktonic foraminifera) zonations, which are commonly used for petroleum exploration wells drilled on the northwestern margin. Revision of the zonations has highlighted a major Upper Campanian to lower Upper Maastrichtian disconformity on the Exmouth Plateau, which went largely unnoticed in previous examinations of the ODP material, but had been recorded previously elsewhere on the northwestern margin. The duration of the disconformity in the Vulcan Sub-basin is unclear, since intervals of the succession may be condensed in this area. *J. Micropalaeontol.* 22(1): 29–62, July 2003.

INTRODUCTION

During the mid–Late Cretaceous, calcareous nannofossil and foraminiferal assemblages on the Western Australian margin (Fig. 1) were differentiated into a high southern-latitude Austral Province, with cool surface-water masses, and a low southern-latitude Tethyan Province with warm surface-water masses (Fig. 2; Rexilius, 1984; Shafik, 1990, 1993; Bralower & Siesser, 1992; Huber, 1992; Wonders, 1992; Watkins *et al.*, 1996). At intermediate latitudes, a Transitional Province existed, with temperate surface waters (Shafik, 1990, 1993; Huber, 1992). Many species of calcareous nannofossil and planktonic foraminifera were cosmopolitan and were present in all three provinces, while others were more temperature-sensitive and confined to a single province. The boundaries between the provinces are diffuse and moved north and south through time, according to global climate, ocean-current circulation, and the position of the Australian continent, which rotated anticlockwise and moved slowly north throughout the Cretaceous (Audley-Charles *et al.*, 1988; Scotese *et al.*, 1988; Metcalfe, 1996).

A global cooling trend commenced during the Late Campanian and continued into the Maastrichtian (Huber *et al.*, 1995; Clarke & Jenkyns, 1999; Premoli Silva & Sliter, 1999). Two brief warming events punctuated this cooling trend, during the mid-Maastrichtian, and again in the very latest Maastrichtian (Barrera, 1994; Huber *et al.*, 1995; Watkins *et al.*, 1996; Barrera *et al.*, 1997). The Western Australian margin spanned *c.* 20° of palaeolatitude during the Maastrichtian, with the Perth and Southern Carnarvon Basins in the south clearly having Austral affinities and the northwestern margin having Transitional affinities (Rexilius, 1984; Shafik 1990, 1993). Maastrichtian strata in Papua New Guinea and northeastern India show strong Tethyan affinities (Shafik, 1990; Chungkham & Jafar, 1998; R. W. Howe, unpublished data).

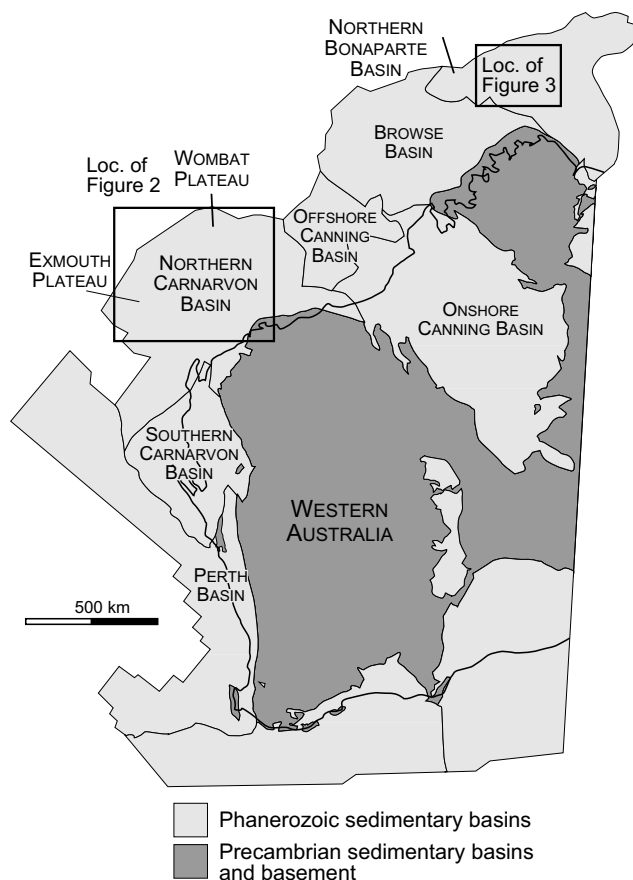


Fig. 1. Location of the studied areas.

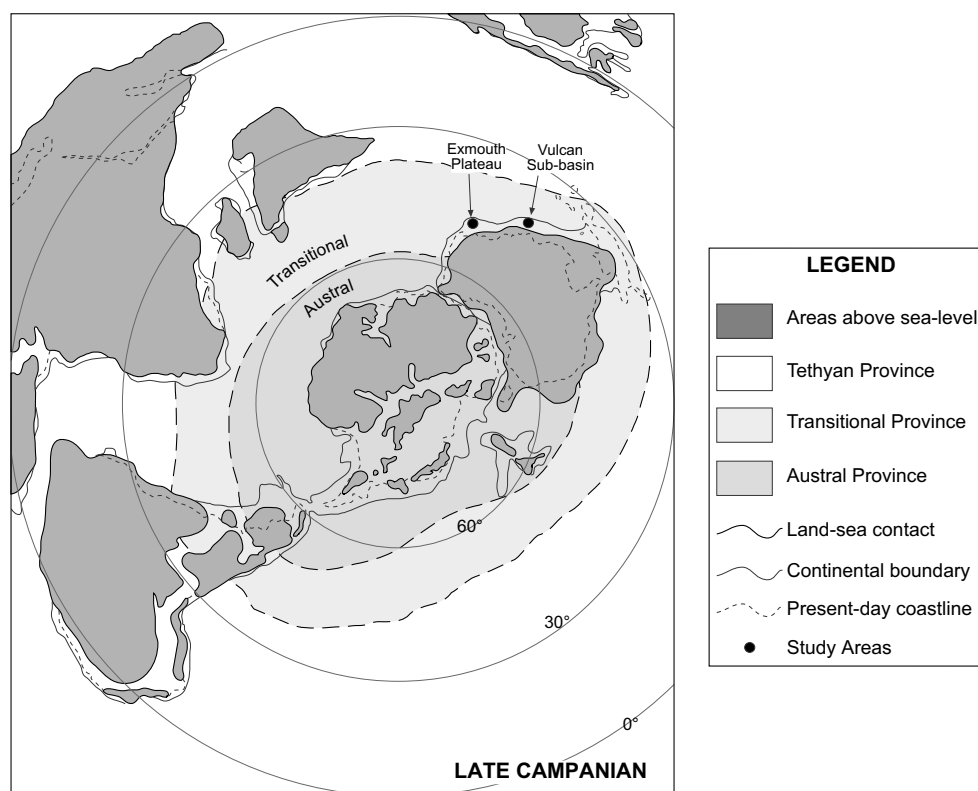


Fig. 2. Palaeogeographical reconstruction for the Late Campanian–Maastrichtian, showing the approximate locations of the studied sections and the inferred palaeobiogeographical boundaries between Austral, Transitional and Tethyan Realms (from Huber, 1992).

This biogeographical differentiation has made biostratigraphic zonation of the Western Australian margin relatively simple during warmer periods where Tethyan influence is greatest (e.g. the latest Albian to Late Santonian) and Tethyan zonations (e.g. Sissingh, 1977 for nannofossils, and Robaszynski & Caron, 1995 for planktonic foraminifera) can be readily applied. During times of cooler surface-water influence (e.g. Aptian to Albian and Campanian to Maastrichtian) Tethyan zonations are more difficult to apply (particularly for planktonic foraminifera), as many index species do not occur, or have different ranges compared to other parts of the world. Bralower & Siesser (1992), Wonders (1992) and Petrizzo (2000) discuss the difficulties of applying both calcareous nannofossil and planktonic foraminiferal Tethyan zonations to the northwestern Australian margin. High-latitude Austral Province zonations (e.g. Watkins *et al.*, 1996 for calcareous nannofossils; Huber, 1991 for planktonic foraminifera) have not been applied to the Western Australian margin, although they would probably be applicable to assemblages in the Perth Basin on the southwestern margin, where Rexilius (1984) records assemblages with strong Austral affinities.

Since the early 1970s studies on the Western Australian margin have either applied local industrial zonations, such as the unpublished KCCM composite foraminiferal and calcareous nannofossil zonation of J. P. Rexilius, which was developed in the early 1980s and the planktonic foraminiferal zonation of Wright & Aphorpe (1976, 1995), or they have used a combination of local and cosmopolitan nannofossil events (e.g. Shafik,

1993). Petroleum exploration companies operating on the northwestern margin of Australia typically employ the KCCM zonation to correlate mid–Upper Cretaceous strata. This zonal scheme uses calcareous nannofossil and foraminiferal events together to provide high-resolution subdivisions, but as the biostratigraphic events that make up the zonation are unpublished, it has been difficult to correlate the KCCM zonation to more widely used global calcareous nannofossil and planktonic foraminiferal zonation schemes (such as the recent UC nannofossil zonation of Burnett, 1998). The present study documents the Maastrichtian part of the KCCM zonation, and introduces a refined version of the zonation, allowing up-to-date correlation of the zonation (and the many petroleum exploration wells on the northwestern Australian margin that are documented in terms of it) to the international chronostratigraphic scale.

STUDY AREA

Tectonic history

The northwestern Australian margin (see Fig. 1) developed as a passive margin following Middle–Late Jurassic rifting of the Gondwana supercontinent (Audley-Charles, 1988; Powell *et al.*, 1988; Baillie *et al.*, 1994; Metcalfe, 1996). Prior to breakup, the northwestern Australian margin was a passive margin on the northeastern edge of Gondwanaland, facing the southern Tethys ocean (von Rad *et al.*, 1992). The onset of rifting and separation of microcontinents from the northwestern Australian margin has been dated as Callovian (Veevers & Powell, 1990), with

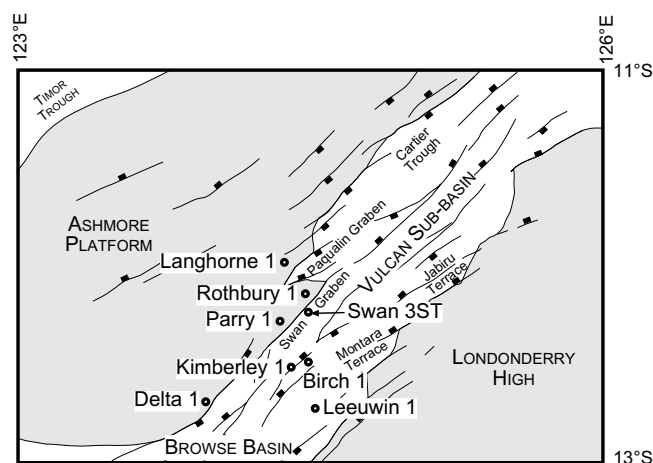


Fig. 3. Location of wells studied in the Browse Basin and Vulcan Sub-basin (after Kennard *et al.*, 1999).

more recent work suggesting an Oxfordian/Kimmeridgian age (Müller *et al.*, 1998). The rifting that had commenced at the northern margin of eastern Gondwanaland propagated southward, separating Greater India from western Australia during the Valanginian, and creating the eastern Indian Ocean (Veevers & Powell, 1990; Holmes & Watkins, 1992; von Rad & Bralower, 1992). By the Maastrichtian (c. 71–65 Ma in the time-scale of Gradstein *et al.*, 1994), the northwestern margin of Australia lay on the eastern side of a mature ocean (see Fig. 2; von Rad *et al.*, 1992), at a palaeolatitude of 30–45°S (Audley-Charles *et al.*, 1988; Struckmeyer *et al.*, 1990; Veevers *et al.*, 1991; Pospichal & Bralower, 1992).

Geological setting

The northwestern margin of Western Australia is segmented into four major sedimentary basins bound by Proterozoic fracture systems: the Bonaparte, Browse, Canning and Carnarvon Basins (O'Brien *et al.*, 1999). This study focuses on the Vulcan Sub-basin in the western Bonaparte Basin (Figs 1, 3), and the Exmouth Plateau in the western part of the Northern Carnarvon Basin (Figs 1, 4). The Vulcan Sub-basin is an elongate (about 270 km long and 80 km wide), northeast–southwest-trending Mesozoic depocentre, comprising a series of horst blocks, grabens and terraces (Kennard *et al.*, 1999). It has fault-bound margins with the Ashmore Platform to the west and the Londonderry High to the east. The structural history of the region is complex, including two extensional events in the Palaeozoic, a compressional event in the Late Triassic and further extension in the Jurassic (O'Brien *et al.*, 1993; Kennard *et al.*, 1999). The Exmouth Plateau is a large, marginal plateau bounded to the east by the Kangaroo Syncline, which separates it from the Beagle Basin, Dampier Sub-basin and Barrow Sub-basin. It is about 600 km long and 300–400 km wide, and is bounded to the north, west and south by the oceanic crust of the Argo, Gascoyne and Cuvier Abyssal Plains, respectively (Exon *et al.*, 1992a).

Stratigraphic framework

Exmouth Plateau. Following Early Cretaceous rifting and the development of a mature ocean on Australia's northwestern

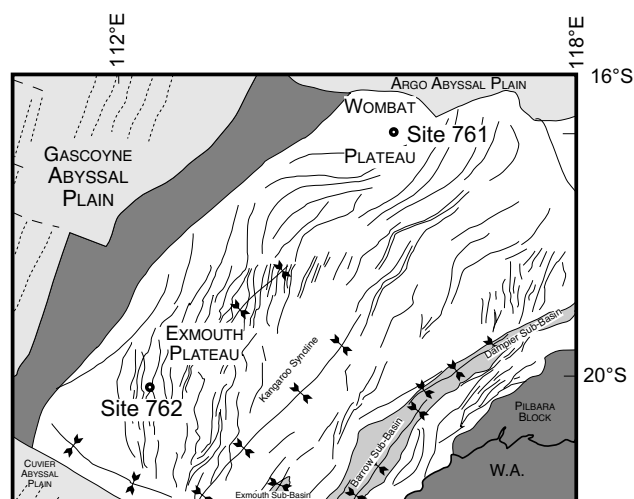


Fig. 4. Location of ODP sites 761 and 762 on the Wombat and Exmouth Plateaus. Structural elements after AGSO North West Shelf Study Group (1994).

margin, the Exmouth Plateau was far from detrital sources, so input of siliciclastic sediment declined (Exon *et al.*, 1992a). As a result, Late Cretaceous and Palaeogene strata are thin and condensed, and consist of chalk and marl successions (Fig. 5). The sediments are typically bioturbated, light green-grey and light brown clayey nannofossil chinks containing foraminifera and ostracods (Haq *et al.*, 1990a, b; Exon *et al.*, 1992b). Huang *et al.* (1992) related cyclic light and dark chalk horizons to orbital changes which controlled the alternation of two prevailing climate regimes in the area. Sedimentation rates at Site 762 were estimated at 14.1 m Ma⁻¹ by Golovchenko *et al.* (1992). Bathyal water depths are interpreted for the Exmouth Plateau

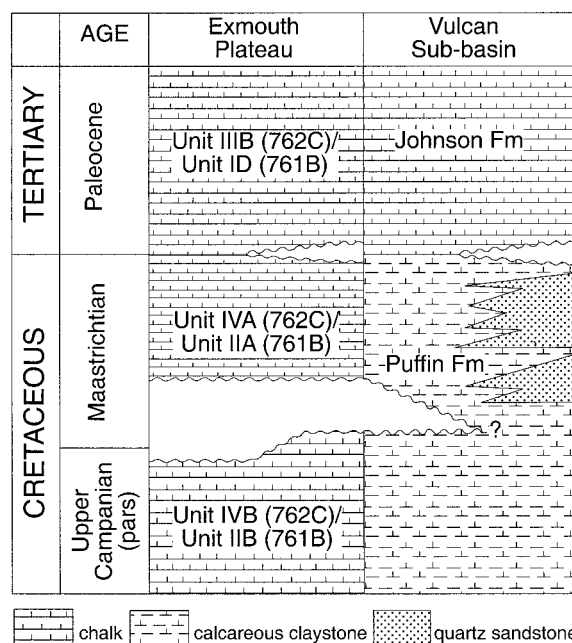


Fig. 5. Lithostratigraphy of the Exmouth Plateau and Vulcan Sub-basin (modified after Exon *et al.*, 1992b and Pattillo & Nicholls, 1990).

Well	Thickness of Maastrichtian sediments	Basin	Latitude (° ' ")	Longitude (° ' ")	Operator
Delta 1	~127m	Browse Basin	12 38 56.4	123 58 13.1	Elf Aquitaine
Langhorne 1	~110.5m	Browse Basin	11 58 46.0	124 21 56.0	TCPL Resources Ltd
ODP Hole 761B	~27m	Exmouth Plateau	16 44 13.80	115 32 6.00	ODP
ODP Hole 762C	~47m	Exmouth Plateau	19 53 13.80	112 15 14.40	ODP
Birch 1	~229m	Vulcan Sub-basin	12 27 33.88	124 29 43.44	BHP Petroleum Pty Ltd
Kimberley 1	~443m	Vulcan Sub-basin	12 36 10.5	124 22 59.11	Norcen International Limited
Leeuwin 1	~259m	Vulcan Sub-basin	12 42 40.35	124 35 06.32	BHP Petroleum Pty Ltd
Parry 1	~195m	Vulcan Sub-basin	12 16 14.33	124 20 15.06	BHP Petroleum Pty Ltd
Rothbury 1	~155m	Vulcan Sub-basin	12 07 35.88	124 28 33.04	TCPL Resources Ltd
Swan 3ST	~275m	Vulcan Sub-basin	12 11 41.36	124 29 37.0	BHP Petroleum Pty Ltd

Table 1. Wells examined in this study.

sections on the basis of the benthonic foraminiferal assemblages which include the species *Aragonia velascoensis*, *Bulimina velascoensis*, *Cibicidoides* spp., *Gaudryina pyramidata*, *Nuttallides truempyi*, *Nuttallinella florealis*, *Pullenia* spp., *Reussella szajnochae*, and *Stensioeina beccariiiformis*, and high planktonic foraminiferal percentages, typically >80%.

Vulcan Sub-basin. Strata of Maastrichtian age in the central and southern Vulcan Sub-basin belong to the Puffin and Borde Formations (Fig. 5). These units reach a maximum thickness of 570 m in the Vulcan Sub-basin, and consist of expanded sections of turbiditic sandstones with interbedded calcareous claystones and marls (Mory, 1988; Pattillo & Nicholls, 1990). The sandstones represent massive channelized submarine fan complexes derived from the southeast (Pattillo & Nicholls, 1990), and are proven petroleum reservoirs (e.g. Puffin 1 and East Swan 1). The benthonic foraminiferal assemblages generally contain diverse rotaliids, lagenids, buliminids and agglutinated taxa, including *Bolivinoidea* spp., *Cibicidoides* spp., *Eouwigierina subsculptura*, *Globorotalites conicus*, *Glomospira charoides*, *Gyroidinoides* spp., *Nuttallinella florealis*, *Osangularia cordieriana*, *Paralabamina* spp., *Praebulimina reussi*, *Pullenia* spp., *Reussella szajnochae* and *Stensioeina beccariiiformis*. These assemblages indicate bathyal depositional environments of more than 200 m, which is supported by a predominance of planktonic foraminifera over benthonic foraminifera within the residues.

MATERIALS AND METHODS

This study is based on material from eight offshore petroleum wells in the Vulcan Sub-basin, and two Ocean Drilling Program (ODP) wells on the Exmouth Plateau (Table 1, Figures 3, 4). The ODP wells were selected because they are continuously cored sections and recovered microfossil assemblages are generally well preserved. The wells from the Vulcan Sub-basin were selected because of expanded Maastrichtian sections and adequate side-wall core spacing. Side-wall core samples were examined from the Vulcan Sub-basin wells at a typical spacing of 10–30 m. Core samples were collected from ODP 761B and ODP 762C at a typical spacing of 1–5 m. The ODP samples were processed for foraminifera using standard preparation techniques (see Glaessner, 1948). These include boiling and

disaggregation of samples in a solution of water, calgon and detergent, and then passing the resulting slurry through a 75 µm mesh sieve. The >75 µm sand fractions were then collected on filter paper in a Buchner funnel, dried and stored in plastic vials. For calcareous nannofossils, smear slides were prepared using the techniques outlined in Perch-Nielsen (1985) and Bown & Young (1998). A small amount of fresh rock was scraped onto a coverslip and then smeared evenly with a wet toothpick. The coverslip was then dried on a hotplate before being glued to a glass slide using Norland optical adhesive.

The Vulcan Sub-basin side-wall core samples had been processed prior to this study by International Stratigraphic Consultants Pty Ltd. All sand-fractions were selectively picked for planktonic foraminifera and biostratigraphically important benthonic foraminifera, and representative specimens were mounted on slides. Nannofossil slides were examined at 1250× magnification using a Zeiss Photomicroscope III cross-polarizing microscope, and taxa were recorded semi-quantitatively. Well-preserved foraminiferal specimens were digitally imaged under the Phillips 505 Scanning Electron Microscope (SEM), having been sputter-coated for 8 minutes with gold at 20–30 mA. Digital images of the nannofossils were captured using a Blue and White Power Macintosh G3/450 and Polaroid DMC 2 digital camera mounted onto the light microscope. All images were imported into Extensis Portfolio 5, a cross-platform image-cataloguing program and are available at <http://www.geol.uwa.edu.au/~biostrat/>, and on CD from the authors. All of the samples and slides used in this study are kept in the calcareous nannofossil and foraminiferal collections in the School of Earth & Geographical Sciences at the University of Western Australia.

RESULTS

Four zonations are outlined below (Fig. 6), the KCN calcareous nannofossil zonation, with seven zones and seven subzones, the KPF planktonic foraminiferal zonation with six zones and five subzones, the KBF benthonic foraminiferal zonation with one zone, and the KCCM composite calcareous microfossil zonation, with eight zones and 11 subzones, which combines the KCN, KPF, and KBF zonations to achieve a robust, high resolution zonation. All of these zonations are modified

STAGE Gradstein et al. (1994), Odin (2001a)	CALCAREOUS NANNOFOSSIL BIOSTRATIGRAPHY					PLANKTONIC FORAMINIFERAL BIOSTRATIGRAPHY			BENTHONIC FORAMINIFERAL BIOSTRATIGRAPHY			COMPOSITE CALCAREOUS MICROFOSSIL BIOSTRATIGRAPHY		
	Sissingh (1977) Perch- Nielsen (1985)	Burnett (1998)	Rexilius (unpubl.)	This study	Nannofossil Events	Robas. & Caron (1995)	Rexilius (unpubl.)	This study	Planktonic Foraminiferal Events	Rexilius (unpubl.)	This study	Benthonic Foraminiferal Events	Rexilius (unpubl.)	This study
MAASTRICHTIAN	CC26	b	a	a	▲ Cretaceous planktonic forams	A. mayaroensis Zone	KPF1 & KPF2	KPF1	▲ Cretaceous planktonic forams	KCCM1	a	▲ Cretaceous planktonic forams	KCCM1	a
		c	b	b	▲ M. prinsii									
		a	a	a	▲ C. kamptneri									
		b	b	b	▲ M. murus									
		a	a	a	▲ L. quadratus									
		b	b	b	▲ A. octoradiata									
		a	a	a	▲ L. praequadratus									
		b	b	b	▲ P. vietus									
		a	a	a	▲ S. coang- uistatus n. sp.									
		b	b	b	▲ Z. birescenticus									
UPPER	CC25	a	a	a	▲ R. levis	G. gansseri Zone	KPF3	KPF3	▲ G. linneiana	KCCM7	a	▲ T. phacelosus	KCCM7	a
		b	b	b	▲ A. parvus constrictus									
		a	a	a	▲ Q. trifidum									
		b	b	b	▲ A. parvus constrictus (Rexilius, unpubl.)									
		a	a	a	▲ B. draco (Rexilius, unpubl.)									
		b	b	b	▲ B. miliaris (Rexilius, unpubl.)									
		a	a	a	▲ B. australis (Rexilius, unpubl.)									
		b	b	b	▲ H. semicostata									
		a	a	a	▲ R. elegans, E. eximius									
		b	b	b	▲ H. semicostata									
LOWER	CC24	b	b	b	▲ T. phacelosus	G. aegyptiaca Zone	KPF4	KPF4	▲ G. linneiana	KCCM8	a	▲ A. parvus constrictus	KCCM8	a
		a	a	a	▲ A. parvus constrictus									
		b	b	b	▲ Q. trifidum									
		a	a	a	▲ A. parvus constrictus (Rexilius, unpubl.)									
		b	b	b	▲ B. draco (Rexilius, unpubl.)									
		a	a	a	▲ B. miliaris (Rexilius, unpubl.)									
		b	b	b	▲ B. australis (Rexilius, unpubl.)									
		a	a	a	▲ H. semicostata									
		b	b	b	▲ R. elegans, E. eximius									
		a	a	a	▲ H. semicostata									
Upper Campanian (pars)	CC23	a	a	a	▲ Q. trifidum	G. aegyptiaca Zone	KPF5	KPF5	▲ G. linneiana	KCCM9	a	▲ A. parvus constrictus	KCCM9	a
		b	b	b	▲ A. parvus constrictus									
		a	a	a	▲ B. draco (Rexilius, unpubl.)									
		b	b	b	▲ B. miliaris (Rexilius, unpubl.)									
		a	a	a	▲ B. australis (Rexilius, unpubl.)									
		b	b	b	▲ H. semicostata									
		a	a	a	▲ R. elegans, E. eximius									
		b	b	b	▲ H. semicostata									
		a	a	a	▲ A. parvus constrictus									
		b	b	b	▲ B. draco (Rexilius, unpubl.)									
Upper Campanian (pars)	CC22	a	a	a	▲ Q. trifidum	G. aegyptiaca Zone	KPF6	KPF6	▲ G. linneiana	KCCM10	a	▲ A. parvus constrictus	KCCM10	a
		b	b	b	▲ A. parvus constrictus									
		a	a	a	▲ B. draco (Rexilius, unpubl.)									
		b	b	b	▲ B. miliaris (Rexilius, unpubl.)									
		a	a	a	▲ B. australis (Rexilius, unpubl.)									
		b	b	b	▲ H. semicostata									
		a	a	a	▲ R. elegans, E. eximius									
		b	b	b	▲ H. semicostata									
		a	a	a	▲ A. parvus constrictus									
		b	b	b	▲ B. draco (Rexilius, unpubl.)									

Fig. 6. Nannofossil, planktonic foraminiferal, benthonic foraminiferal and composite calcareous microfossil zonations of this study compared to previous schemes (Sissingh, 1977; Perch-Nielsen, 1985; Gradstein *et al.*, 1995; Robaszynski & Caron, 1995; Burnett, 1998; Odin, 2001a; Rexilius, unpublished data). The duration of disconformities in the study areas are indicated by shading (dark, Vulcan Sub-basin; light, Exmouth Plateau).

[illegible]

Table 2. Dashed line indicates interpreted position of the Upper Campanian to upper Lower Maastrichtian disconformity (not present in some wells). Abundance is recorded as: VH, very high, >100 specimens per field of view (FOV); H, high, 50–100 specimens per FOV; M, moderate 10–50 specimens per FOV; L, low, 1–10 specimens per FOV; VL, very low, 1 specimen per 1–10 FOVs. Individual species abundances are recorded as follows: A, abundant, >100 specimens per FOV; C, common, 11–100 specimens per FOV; F, few, 1–10 specimens per FOV; R, rare, 1 specimen in 10 FOVs; S, single, only a single specimen observed. As the nannofossil assemblage in a sample can show overgrowth of some species, and dissolution of others, only the overall preservation state of the assemblage is recorded here as: G, good, whole assemblage is well preserved, with the diagnostic features of most species preserved; M, moderate, with some dissolution and/or overgrowth, but most species still identifiable, P, poor, severe dissolution and/or overgrowth, with only a few species identifiable to species level.

[illegible]

Table 2. Continued.

refinements of the unpublished KCN, KPF, KBF and KCCM zonations (see Fig. 5) used by J.P. Rexilius in petroleum exploration work. The KBF benthonic foraminiferal zonation is based on evolutionary lineages within the genus *Bolivinoidea* and is best developed in neritic facies. The lineage is poorly represented in our bathyal material because

of unfavourable facies and, therefore, the KBF zonation was difficult to apply. Comparisons to the CC nannofossil zones of Sissingh (1977) and Perch-Nielsen (1985), the UC nannofossil zones of Burnett (1998), the C planktonic foraminiferal zones of Wright & Apthorpe (1976, 1995), and the revised KCN, KPF and KCCM zones are shown on

[illegible]

Table 2. Continued.

the nannofossil and foraminiferal distribution charts (Tables 2, 3).

Stratigraphic correlation of the KCCM Zonation to the European Campanian and Maastrichtian Stages is mainly based on calcareous nannofossil events. The planktonic foraminiferal assemblages of northwestern Australia are significantly different to those in Europe and the Mediterranean region, since a number of the key markers used in these regions (see Premoli Silva & Sliter, 1994; Robaszynski & Caron, 1995; Odin *et al.* 2001) are either absent or have different ranges in Australia (e.g. *Radotruncana calcarata*). Broad correlations can be made using benthonic foraminiferal events, although the distribution of benthonic species tends to be more facies driven than the distribution of planktonic species.

The Maastrichtian/Campanian boundary GSSP (Global Stratotype Section and Point) was recently ratified by the International Commission on Stratigraphy (ICS) and is located in a disused quarry at Tercis-les-Bains in southwest France (Odin, 2001a). The marker events that define the boundary are the lowest occurrences (LOs) of the Tethyan ammonite *Pachydiscus neubergicus* and the Boreal belemnite *Belemnella lanceolata* (Odin & Lamaurelle, 2001). These events have been correlated to the base of the *Baculites eliasi* ammonite zone in the US Western Interior (Kennedy *et al.*, 1992; Gradstein *et al.*, 1994; Hardenbol & Robaszynski, 1998). The numerical age given for this level by Gradstein *et al.* (1994) is 71.3 ± 0.5 Ma, which is followed in this study, although a numerical age of 72.0 Ma was calibrated for the boundary at Tercis (Odin, 2001b).

Predcosciaphera celatae group spine	CC Zone (Sisalingh, 1977)	UC Zone (Burnett, 1998)	KCN Zone (Rexillius, unpubl.)	Mod. KCN Zone (this study)	Nannofossil Events
Predcosciaphera grandis	CC26b	UC20d	KCN1a	KCN1a	LO M. prinsi
Predcosciaphera majungae	CC25c-26a	UC20b-c	KCN1b-2a	KCN1b-2a	LO M. murus
Predcosciaphera spinosa	CC25b	UC20a	KCN1b-3	KCN2b	LO L. quadratus
Probellatella multicarinata	CC25a	UC19	KCN4a	KCN4a	LO C. gallica
Psudonitella quadrala	CC25b	UC20d	KCN1-3	KCN1-3	LO L. praequadratus, HO A. octoradate, ?HO P. vietus
Psycosphaera finhi	CC25b	UC20d	KCN1-3	KCN1-3	HO S. coangustatus n. sp.
Quadrum bengalensis	CC25b	UC20d	KCN1-3	KCN1-3	HO R. levis, Z. horrescenticus
Quadrum gothicum	CC25b	UC20d	KCN1-3	KCN1-3	HO A. parvus ssp. constrictus
Quadrum trifidum	CC25b	UC20d	KCN1-3	KCN1-3	not zoned
Reinhardtites levis	CC25b	UC20d	KCN1-3	KCN1-3	LO M. prinsi
Retecapsa schizobrachiala	CC25b	UC20d	KCN1-3	KCN1-3	?LO M. prinsi
Retecapsa spp.	CC25b	UC20d	KCN1-3	KCN1-3	LO L. quadratus
Rhagodiscus angustus	CC25b	UC20d	KCN1-3	KCN1-3	LO L. praequadratus, C. gallica, ?HO P. vietus
Rhagodiscus plebius	CC25b	UC20d	KCN1-3	KCN1-3	HO S. coangustatus n. sp.
Rhagodiscus reniformis	CC25b	UC20d	KCN1-3	KCN1-3	HO R. levis, Z. horrescenticus
Rhagodiscus splendens	CC25b	UC20d	KCN1-3	KCN1-3	HO A. parvus ssp. constrictus
Rotellipilus laffitei	CC25b	UC20d	KCN1-3	KCN1-3	not zoned
Rucinolitus sp. 8	CC25b	UC20d	KCN1-3	KCN1-3	LO L. quadratus
Rucinolitus hayi	CC25b	UC20d	KCN1-3	KCN1-3	LO L. praequadratus, C. gallica, ?HO P. vietus
Russellia buryi	CC25b	UC20d	KCN1-3	KCN1-3	HO S. coangustatus n. sp.
Scapanella spp.	CC25b	UC20d	KCN1-3	KCN1-3	HO R. levis, Z. horrescenticus
Semiholothius priscus	CC25b	UC20d	KCN1-3	KCN1-3	HO A. parvus ssp. constrictus
Staurolithes ellipticus	CC25b	UC20d	KCN1-3	KCN1-3	not zoned
Staurolithes imbricatus	CC25b	UC20d	KCN1-3	KCN1-3	LO L. quadratus
Staurolithes laffitei	CC25b	UC20d	KCN1-3	KCN1-3	LO L. praequadratus, C. gallica, ?HO P. vietus
Staurolithes meliense	CC25b	UC20d	KCN1-3	KCN1-3	HO S. coangustatus n. sp.
Staurolithes stradneri	CC25b	UC20d	KCN1-3	KCN1-3	HO R. levis, Z. horrescenticus
Stoverius coangustatus n. sp.	CC25b	UC20d	KCN1-3	KCN1-3	HO A. parvus ssp. constrictus
Tegumentum stradneri	CC25b	UC20d	KCN1-3	KCN1-3	not zoned
Tetrapodiorhabdus decorus coccolith	CC25b	UC20d	KCN1-3	KCN1-3	LO L. quadratus
Tetrapodiorhabdus decorus spine	CC25b	UC20d	KCN1-3	KCN1-3	LO L. praequadratus, C. gallica, ?HO P. vietus
Tetrapodiorhabdus decorus	CC25b	UC20d	KCN1-3	KCN1-3	HO S. coangustatus n. sp.
Tranolitus phaeobius	CC25b	UC20d	KCN1-3	KCN1-3	HO R. levis, Z. horrescenticus
Watznaueria barnesae	CC25b	UC20d	KCN1-3	KCN1-3	HO A. parvus ssp. constrictus
Watznaueria ovata	CC25b	UC20d	KCN1-3	KCN1-3	not zoned
Zeughrabodius bicrescenticus	CC25b	UC20d	KCN1-3	KCN1-3	LO L. quadratus
Zeughrabodius embergeri	CC25b	UC20d	KCN1-3	KCN1-3	LO L. praequadratus, C. gallica, ?HO P. vietus
Zeughrabodius minimus	CC25b	UC20d	KCN1-3	KCN1-3	HO S. coangustatus n. sp.
Zeughrabodius praesignoides	CC25b	UC20d	KCN1-3	KCN1-3	HO R. levis, Z. horrescenticus
Zeughrabodius spiralis	CC25b	UC20d	KCN1-3	KCN1-3	HO A. parvus ssp. constrictus
Zeughrabodius taboulensis	CC25b	UC20d	KCN1-3	KCN1-3	not zoned
Zeughrabodius cf. trivectis	CC25b	UC20d	KCN1-3	KCN1-3	LO L. quadratus
Zeughrabodius wynnai	CC25b	UC20d	KCN1-3	KCN1-3	LO L. praequadratus, C. gallica, ?HO P. vietus

Table 2. Continued.

At Tercis, calcareous nannofossil, planktonic foraminiferal, and benthonic foraminiferal events have been tied to the LO of *Pachydiscus neubergicus*. Studies by von Salis (2001), Gardin & Monechi (2001) and Melinte & Odin (2001) show that the HO (highest occurrence) of the nannofossil *Aspidolithus parvus constrictus* occurs significantly above the Maastrichtian/Campanian boundary, in contrast to earlier correlations that placed the event slightly below the boundary (Burnett *et al.*, 1992a; Burnett, 1998). The HO of *Quadrum trifidum* is located above the boundary, below the HO of *A. p. constrictus*, while the HOs of *Eiffelithus eximius* and *Reinhardtites anthophorus* were shown to be slightly below the boundary (Gardin *et al.*, 2001).

The LO of *P. neubergicus* has been shown to occur well above the HO of the planktonic foraminiferal marker *Radotruncana calcarata* (Premoli Silva & Sliter, 1994; Robaszynski & Caron,

1995; Ion & Odin, 2001) and correlated to within the *Gansserina gansseri* Zone (Robaszynski *et al.*, 1984; Premoli Silva & Sliter, 1994). It is interesting that at Tercis the LO of *G. gansseri* occurs above the Maastrichtian–Campanian boundary (Odin *et al.*, 2001), suggesting that the appearance of this species may be diachronous. In terms of benthonic foraminifera, *Bolivinooides* cf. *australis* was recorded above the Maastrichtian–Campanian boundary at Tercis, while *B. miliaris* ranged from the uppermost Campanian to the lower Lower Maastrichtian (Tronchetti, 2001). Tronchetti *et al.* (2001) note a change at the Campanian–Maastrichtian boundary from *Bolivinooides* taxa with four lobes on the suture of the final chambers to specimens with five lobes above the boundary. In this study we have correlated the LO of *Bolivinooides australis* to approximate the Campanian–Maastrichtian boundary, following Robaszynski

Well	Depth (m)	Sample Type & Number	Foraminiferal Abundance	Foraminiferal Preservation	Turbiditic sand horizons	Foraminiferal Species
Birch-1	1979.2	swc 120	B	-	sand	1 <i>Albafomphalus intermedius</i>
	1987.3	swc 116	H	P		2 <i>Albafomphalus mayroensis</i>
	1988.5	swc 115	M-H	P		3 <i>Contusotruncana confusa</i>
	1989.2	swc 114	VL	VP		4 <i>Contusotruncana cf. contusa</i>
	2005.0	swc 111	H	P-M		5 <i>Contusotruncana loricata</i>
	2015.0	swc 110	H	P-M		6 <i>Contusotruncana cf. loricata</i>
	2048.0	swc 97	M	P-M		7 <i>Contusotruncana cf. paleiformis</i>
	2054.0	swc 95	L-M	P		8 <i>Contusotruncana cf. plicata</i>
	2057.5	swc 94	H	P		9 <i>Contusotruncana walfischensis</i>
	2076.0	swc 92	H	P		10 <i>Contusotruncana sp. indet.</i>
	2090.3	swc 91	VH	P-M		11 <i>Globigerrhella cf. alvarezii</i>
	2104.0	swc 143	M	P-M		12 <i>Globigerrhella multipina</i>
	2141.8	swc 87	M	P-M		13 <i>Globigerrhella praeinhiensis</i>
	2161.5	swc84	M	P-M		14 <i>Globigerrhella subcarinatus</i>
	2184.8	swc81	M	P		15 <i>Globigerrhella ultranica</i>
Delta-1	2208.0	swc79	H-VH	P-M		16 <i>Globotruncana cf. aegyptiaca</i>
	2748.0	swc8	M-H	VP		17 <i>Globotruncana anza</i>
	2834.0	swc6	L-M	XP		18 <i>Globotruncana bulboides</i>
	2867.5	swc4	M-H	VP		19 <i>Globotruncana cf. bulboides</i>
	2875.0	swc1	M-H	VP		20 <i>Globotruncana dupeblei</i>
Kimberley-1	1850.0	swc	B	-	sand	21 <i>Globotruncana cf. esenheims</i>
	1855.0	swc	B	-	sand	22 <i>Globotruncana faustianii</i>
	1860.0	swc	VL	P		23 <i>Globotruncana cf. insignis</i>
	1865.0	swc	B	-	sand	24 <i>Globotruncana linneiana</i>
	1881.0	swc	B	-	sand	25 <i>Globotruncana linneiana (reworked)</i>
	1895.0	swc	B	-	sand	26 <i>Globotruncana cf. linneiana</i>
	1907.0	swc	B	-	sand	27 <i>Globotruncana orientalis</i>
	1920.0	swc	B	-	sand	28 <i>Globotruncana rigosa</i>
	1950.0	swc	H	P-M		29 <i>Globotruncana ventricosa</i>
	1965.0	swc	H	P		30 <i>Globotruncana cf. ventricosa</i>
	1980.0	swc	VL	P		31 <i>Globotruncana sp. (spines)</i>
	2005.0	swc	L	VP		32 <i>Globotruncana sp. A</i>
	2030.0	swc	B	-	sand	33 <i>Globotruncanella havanensis</i>
	2055.0	swc	B	-	sand	34 <i>Globotruncanella petaloides</i>
	2065.0	swc	M-H	P-M		35 <i>Globotruncanella cf. petaloides</i>
Langhorne-1	2100.0	swc	B	-	sand	36 <i>Globotruncanella angulata</i>
	2155.0	swc	B	-	sand	37 <i>Globotruncanella sp. indet.</i>
	2180.0	swc	B	-	sand	38 <i>Globotruncanella cf. conica</i>
	2210.0	swc	B	-	sand	39 <i>Globotruncanella cf. petterii</i>
	2225.0	swc	M-H	P		40 <i>Globotruncanella stuarti</i>
	2240.0	swc	M-H	P		41 <i>Globotruncanella sp. A</i>
	2280.0	swc	L	P-M		42 <i>Globotruncanella sp. indet.</i>
	2293.0	swc	B	-	sand	43 <i>Gublerina acuta</i>
	2292.5	swc	L-M	P		44 <i>Gublerina cunilieri</i>
	2316.0	swc	M	P-M		45 <i>Guembellina cretacea</i>
Leeuwin-1	2324.0	swc	M	P-M		46 <i>Hedbergella cf. holmdensis</i>
	2354.0	swc	H	P-M		47 <i>Heterohelix globulosa</i>
	2371.0	swc	M-H	P		48 <i>Heterohelix planata</i>
	2386.5	swc	H	P		49 <i>Heterohelix cf. punctulata</i>
	2395.0	swc	H	VP-P		50 <i>Heterohelix rajagopalani</i>
	2406.0	swc	H	VP		51 <i>Heterohelix semicostata</i>
	1635.0	swc	H	P-M		52 <i>Laeviheterohelix dentata</i>
	1639.0	swc	H	P-M		53 <i>Laeviheterohelix glabrans</i>
	1653.0	swc	H	P		
	1684.5	swc	B	-	sand	
ODP-761B	1733.0	swc	H	P		
	1745.0	swc	H	VP-P		
	1843.0	swc	B	-	sand	
	1851.0	swc	M	VP-P		
	1868.0	swc	M-H	P-M		
	1894.0	swc	M-H	P		
	176.1	21X-4, 144-145 cm	H	G		
	177.6	21X-5, 140-141 cm	VH	G		
	180.8	22X-1, 112-113 cm	M	M-G		
	183.9	22X-3, 115-115 cm	M	M-G		
	186.8	22X-5, 106-107 cm	M	M-G		
	189.4	23X-1, 20-21 cm	M-H	M		
	191.8	23X-2, 110-111 cm	M	M		
	195.3	23X-5, 5-6 cm	VH	G		
	199.8	24X-1, 110-111 cm	VH	G		
	201.3	24X-2, 110-111 cm	VH	M-G		
	202.7	24X-3, 95-96 cm	M-H	M-G		
	209.4	25X-1, 120-121 cm	VH	G		
	210.9	25X-2, 105-106 cm	H-VH	M-G		
	213.9	25X-4, 120-121 cm	H	M		

Table 3. Dashed line indicates interpreted position of the Upper Campanian to upper Lower Maastrichtian disconformity (not present in some wells). Abundance is recorded as: A, abundant (>50 specimens per sample); C, common (20–50 specimens per sample); F, frequent (10–19 specimens per sample); R, rare (2–9 specimens per sample); and S, single (1 specimen per sample). Preservation is recorded as: G, good; M, moderate; and P, poor, and was dependent on the level of recrystallization, overgrowth and/or dissolution. Asterisk denotes probably caved specimens

54 <i>Magnituncana coronata</i> (reworked) 55 <i>Magnituncana marginata</i> (reworked) 56 <i>Planoglobulina acervulinoides</i> 57 <i>Planoglobulina cf. carseyae</i> 58 <i>Planoglobulina multicamerata</i> 59 <i>Planoglobulina rogersensis</i> 60 <i>Pseudoglobulina costulata</i> 61 <i>Pseudoglobulina excolata</i> 62 <i>Pseudoglobulina palpebra</i> 63 <i>Pseudotextularia cushmani</i> 64 <i>Pseudotextularia elegans</i> 65 <i>Pseudotextularia intermedia</i> 66 <i>Pseudotextularia cf. intermedia</i> 67 <i>Reconigumbelina fructuosa</i> 68 <i>Reconigumbelina powelli</i> 69 <i>Rugoglobbigerina hexacamerata</i> 70 <i>Rugoglobbigerina milamensis</i> 71 <i>Rugoglobbigerina pennyi</i> 72 <i>Rugoglobbigerina rotundata</i> 73 <i>Rugoglobbigerina rugosa</i> 74 <i>Rugituncana cf. subcircummodifera</i> <i>Bolivinoidea</i> spp. 75 <i>Bolivinoidea australis</i> 76 <i>Bolivinoidea delicatulus</i> 77 <i>Bolivinoidea draco</i> 78 <i>Bolivinoidea cf. draco</i> 79 <i>Bolivinoidea giganteus</i> 80 <i>Bolivinoidea miliaris</i> 81 <i>Bolivinoidea sp. indet.</i> <i>Stensioelina</i> spp. 82 <i>Stensioelina pommerana</i> Tertiary Planktonics (caved) <i>Globbigerina trilobuloides</i> 83	Wright & Aphorpe (1976; 1995)	KPF Zone (Rexilius, unpub.)	Mod. KPF Zone (this study)	KBF Zone (Rexilius, unpub.)	Mod. KCCM Zone (this study)	Events
R	Indet.	Indet.	Indet.	Indet.	KCCM1	
R	C13	KPF1-2	KPF1a	KBF1	KCCM1-2a	
F	Indet.	Indet.	Indet.	Indet.	Indet.	
S					KCCM1	
R					KCCM1-2a	
R	C13	KPF1-2	KPF1a	KBF1	KCCM1	LO <i>G. dupeublei</i>
R					KCCM1-2	LO <i>B. draco</i>
R					KCCM1-2	LO <i>C. contusa</i> , <i>R. fructuosa</i> , <i>R. powelli</i> , <i>P. intermedia</i> , <i>P. elegans</i> , <i>G. stuarti</i>
R					KCCM5	LO <i>G. angulata</i>
R					KCCM5	LO <i>A. mayaroensis</i> , <i>P. acervulinoides</i> , <i>P. palpebra</i>
R					KCCM5b	LO <i>G. cuvillieri</i> ?, HO <i>S. pommerana</i>
R	Indet.	KPF3	KPF3?	Indet.	KCCM8b	
R	Indet.	Indet.	Indet.	Indet.	not zoned	LO <i>P. cushmani</i> ?, HO <i>G. linneiana</i>
R	C13?	KPF1/2?	KPF2b? +		?KCCM7-8a	
R	Indet.	Indet.	Indet.	Indet.	Indet.	HO <i>S. pommerana</i>
R	C13?	KPF1/2?	Indet.	Indet.	KCCM8b +	LO <i>A. mayaroensis</i> ?, <i>G. cuvillieri</i>
R?	Indet.	KPF4-5	KPF4-5	Indet.	not zoned	HO <i>G. linneiana</i>
S	Indet.	Indet.	Indet.	Indet.	Indet.	
S	C13	KPF1-2	KPF1	Indet.	KCCM1a	
R	Indet.	Indet.	Indet.	Indet.	Indet.	
R	Indet.	Indet.	Indet.	Indet.	KCCM1-2	
R	Indet.	Indet.	Indet.	Indet.	Indet.	
R	Indet.	Indet.	Indet.	Indet.	KCCM1-2a	
R	Indet.	Indet.	Indet.	Indet.	KCCM1-2	
R	Indet.	Indet.	Indet.	Indet.	KCCM1-2	
R	Indet.	Indet.	Indet.	Indet.	Indet.	
R	C13	KPF1-2	KPF1	KBF1	KCCM1-2	LO <i>P. acervulinoides</i>
R	Indet.	Indet.	Indet.	Indet.	Indet.	
R	C13	KPF1-2	KPF1	KBF1	KCCM1-2	LO <i>C. walfischensis</i> , <i>G. dupeublei</i>
R	Indet.	Indet.	Indet.	Indet.	KCCM5	LO <i>R. fructuosa</i> , <i>R. powelli</i> , <i>G. stuarti</i> , <i>P. palpebra</i>
R	Indet.	Indet.	Indet.	Indet.	Indet.	LO <i>A. mayaroensis</i> , <i>G. angulata</i> , <i>B. draco</i>
R	Indet.	Indet.	Indet.	Indet.	KCCM1-2a	
R	C13	KPF1-2	KPF1a	KBF1	KCCM1-2	LO <i>P. elegans</i> , <i>R. fructuosa</i> , <i>P. palpebra</i> , <i>C. contusa</i>
R	Indet.	Indet.	Indet.	Indet.	KCCM5	LO <i>B. draco</i> , <i>P. acervulinoides</i> ?
R	Indet.	Indet.	Indet.	Indet.	KCCM6b	LO <i>A. mayaroensis</i> , <i>G. stuarti</i> , <i>P. intermedia</i> , <i>R. powelli</i>
R	Indet.	Indet.	Indet.	Indet.	KCCM6e	LO <i>B. miliaris</i> , <i>G. cuvillieri</i> , HO <i>S. pommerana</i>
R	C11	KPF4-5	KPF4-5	Indet.	not zoned	HO <i>G. linneiana</i>
R	C13	KPF1-2	KPF1a	KBF1	KCCM1-2	
R	Indet.	Indet.	Indet.	Indet.	Indet.	
R	C13	KPF1-2	KPF1a	KBF1	KCCM1-2	LO <i>A. mayaroensis</i> , <i>C. contusa</i> , <i>P. acervulinoides</i> , <i>P. palpebra</i>
R	C12	KPF2	KPF1b	KBF1	KCCM4	LO <i>R. fructuosa</i> , <i>C. walfischensis</i> , <i>B. draco</i> , <i>G. angulata</i> , <i>P. elegans</i> , <i>R. powelli</i> , <i>P. intermedia</i> , <i>R. stuarti</i>
R	Indet.	Indet.	Indet.	Indet.	KCCM6a	
R	Indet.	Indet.	Indet.	Indet.	KCCM6e	LO <i>G. cuvillieri</i>
R	C11	KPF4-5	KPF4-5	Indet.	not zoned	HO <i>G. linneiana</i>
R	C13	KPF1-2	KPF1a	KBF1	KCCM1-2a	LO/HO <i>B. australis</i>
R	Indet.	Indet.	Indet.	Indet.	KCCM1a	
R	Indet.	Indet.	Indet.	Indet.	KCCM1-2a	
R	Indet.	Indet.	Indet.	Indet.	KCCM2b	LO <i>C. contusa</i>
R	Indet.	Indet.	Indet.	Indet.	KCCM5	LO <i>R. fructuosa</i>
R	Indet.	Indet.	Indet.	Indet.	KCCM5b	LO <i>P. palpebra</i> , <i>P. acervulinoides</i>
R	Indet.	Indet.	Indet.	Indet.	KCCM6c	LO <i>G. angulata</i> , <i>R. powelli</i>
R	Indet.	Indet.	Indet.	Indet.	KCCM6b-f	LO <i>A. mayaroensis</i> , HO <i>S. pommerana</i>
R	Indet.	Indet.	Indet.	Indet.	KCCM6b-f	LO <i>G. cuvillieri</i> , <i>P. elegans</i> , <i>P. intermedia</i> , <i>G. stuarti</i> , <i>A. intermedia</i> ?
R	C10	KPF6	KPF6	Indet.	not zoned	HO <i>H. semicostata</i> , <i>G. linneiana</i>
R						LO <i>H. semicostata</i> , <i>P. cushmani</i>

Table 3. Continued.

Well	Depth (m)	Sample Type & Number	Foraminiferal Abundance	Foraminiferal Preservation	Turbiditic sand horizons	Foraminiferal Species
ODP-762C	555.5	43X-1, 95-96 cm	H	M-G		<i>Alabonophalus intermedius</i>
	559.5	43X-4, 45-46 cm	VH	M-G		<i>Alabonophalus mayaroensis</i>
	564.9	44X-1, 85-86 cm	H	M		<i>Contusotruncana contusa</i>
	569.3	44X-4, 84-85 cm	H	M		<i>Contusotruncana cf. contusa</i>
	572.2	44X-6, 86-87 cm	H	M-G		<i>Contusotruncana fomicata</i>
	576.0	45X-2, 100-101 cm	H	M		<i>Contusotruncana cf. fomicata</i>
	579.3	45X-4, 127-128 cm	H	M		<i>Contusotruncana cf. plicata</i>
	584.0	46X-1, 97-98 cm	VH	G		<i>Contusotruncana wellischensis</i>
	587.2	46X-3, 116-117 cm	VH	M-G		<i>Contusotruncana sp. indet.</i>
	593.6	47X-1, 107-108 cm	VH	M		<i>Globobulimina cf. alvarezii</i>
	595.7	47X-3, 22-23 cm	VH	G		<i>Globobulimina multispinosa</i>
	599.6	47X-5, 106-107 cm	H	M		<i>Globobulimina praehellicensis</i>
	600.6	47X-6, 80-81 cm	VH	M-G		<i>Globobulimina subcarinata</i>
	601.7	47X-7, 16-17 cm	VH	M-G		<i>Globobulimina ultramica</i>
	603.0	48X-1, 96-97 cm	H-VH	M		<i>Globobulimina cf. aegyptiaca</i>
	604.4	48X-2, 93-94 cm	VH	M-G		<i>Globobulimina arca</i>
	606.9	48X-4, 40-41 cm	VH	M		<i>Globobulimina bulloides</i>
	610.3	48X-6, 75-76 cm	VH	M-G		<i>Globobulimina cf. bulloides</i>
	611.2	48X-7, 16-17 cm	VH	M-G		<i>Globobulimina dupoulei</i>
	2164.5	swc 91	B	P	sand	<i>Globobulimina cf. senhensis</i>
	2167.2	swc 89	M	P-M		<i>Globobulimina falsostuani</i>
	2173.0	swc 82	M	P-M		<i>Globobulimina cf. insignis</i>
	2176.7	swc 79	M	P		<i>Globobulimina limeliana (rewired)</i>
Parry-1	2178.5	swc 38	M	P-M		<i>Globobulimina cf. limeliana</i>
	2188.5	swc 78	M	P		<i>Globobulimina cf. ventricosa</i>
	2194.0	swc 35	H	P		<i>Globobulimina sp. (spines)</i>
	2201.0	swc 34	H	P		<i>Globobulimina sp. A</i>
	2209.0	swc 77	H	P-M		<i>Globobuliminella havensis</i>
	2220.5	swc 76	M	P-M		<i>Globobuliminella petaloidea</i>
	2224.0	swc 30	H	P-M		<i>Globobuliminella cf. petaloidea</i>
	2229.5	swc 75	B	P	sand	<i>Globobuliminella sp. indet.</i>
	2256.0	swc 74	M	P-M		<i>Globobuliminella angulata</i>
	2256.0	swc 74	M	P-M		<i>Globobuliminella cf. conica</i>
	2256.0	swc 74	M	P-M		<i>Globobuliminella cf. pettersi</i>
	2256.0	swc 74	M	P-M		<i>Globobuliminella stuarti</i>
Rothbury-1	2495.0	swc	H	P		<i>Globobuliminella sp. A</i>
	2503.0	swc	H	P		<i>Globobuliminella petaloidea</i>
	2515.0	swc	H	P		<i>Globobuliminella cf. petaloidea</i>
	2527.0	swc	H	P		<i>Globobuliminella sp. indet.</i>
	2545.0	swc	M-H	P		<i>Globobuliminella angulata</i>
	2565.0	swc	H	VP		<i>Gublerina acuta</i>
	2577.0	swc	M	VP		<i>Gublerina cuvieri</i>
	2590.0	swc	M	P		<i>Gublerina cuvieri</i>
	2603.0	swc	M-H	VP-P		<i>Gublerina cuvieri</i>
	2615.0	swc	H	VP		<i>Gublerina cuvieri</i>
	2627.0	swc	L-M	P		<i>Gublerina cuvieri</i>
	2640.0	swc	H	P		<i>Gublerina cuvieri</i>
Swan-3ST	2650.0	swc	H	P		<i>Gublerina cuvieri</i>
	2150.0	swc 57-3	H	P		<i>Gublerina cuvieri</i>
	2200.0	swc 56-3	H	P		<i>Gublerina cuvieri</i>
	2240.0	swc 54-3	H	P		<i>Gublerina cuvieri</i>
	2280.0	swc 52-3	H	P		<i>Gublerina cuvieri</i>
	2300.0	swc 51-3	H	P		<i>Gublerina cuvieri</i>
	2310.0	swc 50-3	H	P		<i>Gublerina cuvieri</i>
	2320.0	swc 49-3	H	P		<i>Gublerina cuvieri</i>
	2330.0	swc 48-3	M	P		<i>Gublerina cuvieri</i>
	2339.0	swc 47-3	H	P		<i>Gublerina cuvieri</i>
	2345.0	swc 46-3	B	VP	sand	<i>Gublerina cuvieri</i>
	2350.0	swc 45-3	VL	VP	sand	<i>Gublerina cuvieri</i>
	2352.0	swc 44-3	M	P		<i>Gublerina cuvieri</i>
	2354.5	swc 43-3	L	P		<i>Gublerina cuvieri</i>
	2356.0	swc 42-3	B	P	sand	<i>Gublerina cuvieri</i>
	2361.0	swc 40-3	M	P		<i>Gublerina cuvieri</i>
	2364.5	swc 39-3	B	P	sand	<i>Gublerina cuvieri</i>
	2368.0	swc 37-3	B	P	sand	<i>Gublerina cuvieri</i>
	2373.5	swc 33-3	B	P	sand	<i>Gublerina cuvieri</i>
	2385.0	swc 30-3	L-M	P		<i>Gublerina cuvieri</i>
	2395.0	swc 28-3	M	P		<i>Gublerina cuvieri</i>
	2405.0	swc 26-3	M	P		<i>Gublerina cuvieri</i>
	2415.0	swc 24-3	M-H	P		<i>Gublerina cuvieri</i>
	2425.0	swc 22-3	M	P-M		<i>Gublerina cuvieri</i>

Table 3. Continued.

et al. (1984) and in agreement with the lobe observations of Tronchetti *et al.* (2001).

The subdivision of the Maastrichtian Stage into Upper and Lower substages is informal. The candidate GSSP for

the substage boundary is the section at Zumaya, northern Spain (Odin, 1996). Potential markers for the substage boundary include the HO of rudistid reefs, the HO of the majority of inoceramids, and the LO of the ammonite

Table 3. Continued.

1994a) and nannofossil data (Burnett *et al.*, 1992b) indicates that the LO of *P. gollevillensis* occurs just below the HO of the inoceramids, within Zones CC24–25a, and in the upper *Gansserina gansseri* Zone. In contrast, the LO of *P. fresvillensis* occurs a lot lower in the succession, within the *G. gansseri* Zone and in upper CC23B (Ward & Kennedy, 1993; MacLeod, 1994a).

Calcareous nannofossil biostratigraphy

All taxa referred to in this section are illustrated in Plates 1–4.

Zone KCN1

Definition. Interval from the HO of Cretaceous planktonic foraminifera to the LO of *Ceratolithoides kamptneri*. Upper Cretaceous nannofossils are abundantly reworked into lower Danian sediments on the northwestern Australian margin (JPR, unpublished data), so the HO of Cretaceous nannofossils is not a useful event for marking the top of the Maastrichtian. The HO of Cretaceous planktonic foraminifera, which are much less easily reworked, is a preferred event and is used in this study.

Age. Late Late Maastrichtian.

Remarks. In this study, *C. kamptneri* is rare and sporadic in occurrence.

Subzone KCN1a

Definition. Interval from the HO of Cretaceous planktonic foraminifera to the LO of *Micula prinsii*.

Age. Latest Maastrichtian.

Remarks. In this study, *M. prinsii* is rare and sporadic in occurrence. *Cribrosphaerella daniae* and *Nephrolithus frequens* are sometimes present in association with *M. prinsii*, particularly in ODP Holes 761B and 762C, and are used as proxies to indicate this subzone in the absence of *M. prinsii*.

Subzone KCN1b

Definition. Interval from the LO of *Micula prinsii* to the LO of *Ceratolithoides kamptneri*.

Age. Late Late Maastrichtian.

Zone KCN2

Definition. Interval from the LO of *Ceratolithoides kamptneri* to the LO of *Lithraphidites quadratus s. s.*

Age. Middle Late Maastrichtian.

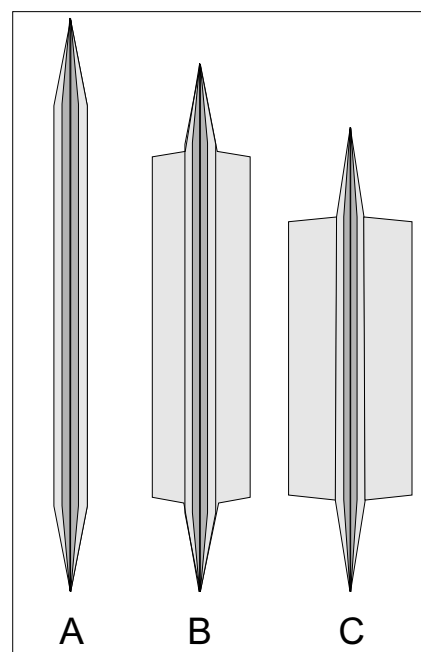


Fig. 7. Morphological criteria of Roth (1978) for the separation of (A) *Lithraphidites carniolensis* (Length/Width ratio ≥ 5), (B) *L. praequadratus* ($3.5 < \text{Length/Width ratio} < 5$), and (C) *L. quadratus* (Length/Width ratio ≤ 3.5).

Remarks. In this study, *Lithraphidites quadratus* and *L. praequadratus* have been separated morphometrically following the criteria of Roth (1978); Figure 7.

Subzone KCN2a

Definition. Interval from the LO of *Ceratolithoides kamptneri* to the LO of *Micula murus*.

Age. Middle Late Maastrichtian.

Remarks. In this study, *M. murus* is rare and sporadic in occurrence.

Subzone KCN2b

Definition. Interval from the LO of *Micula murus* to the LO of *Lithraphidites quadratus s. s.*

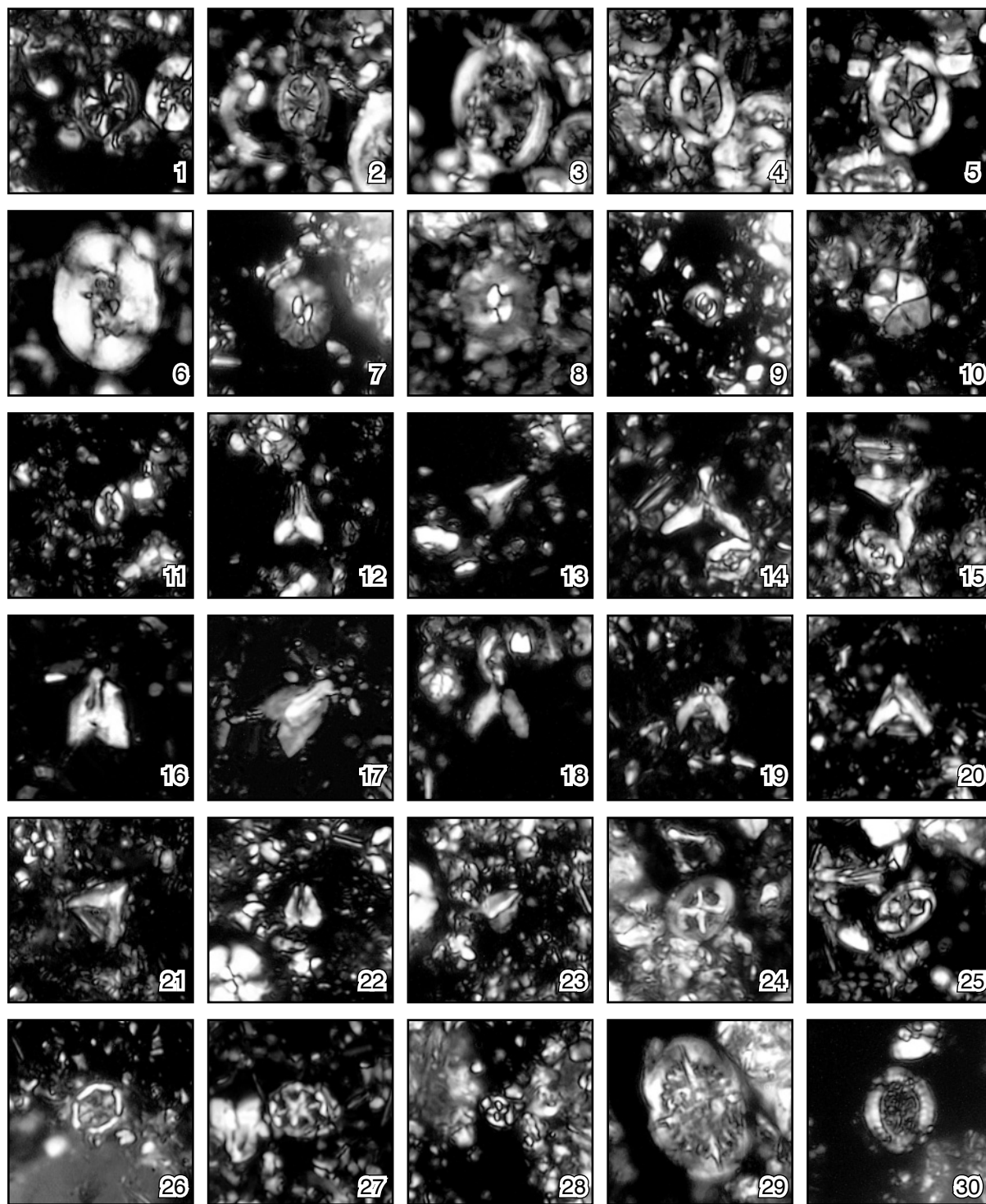
Age. Middle Late Maastrichtian.

Zone KCN3

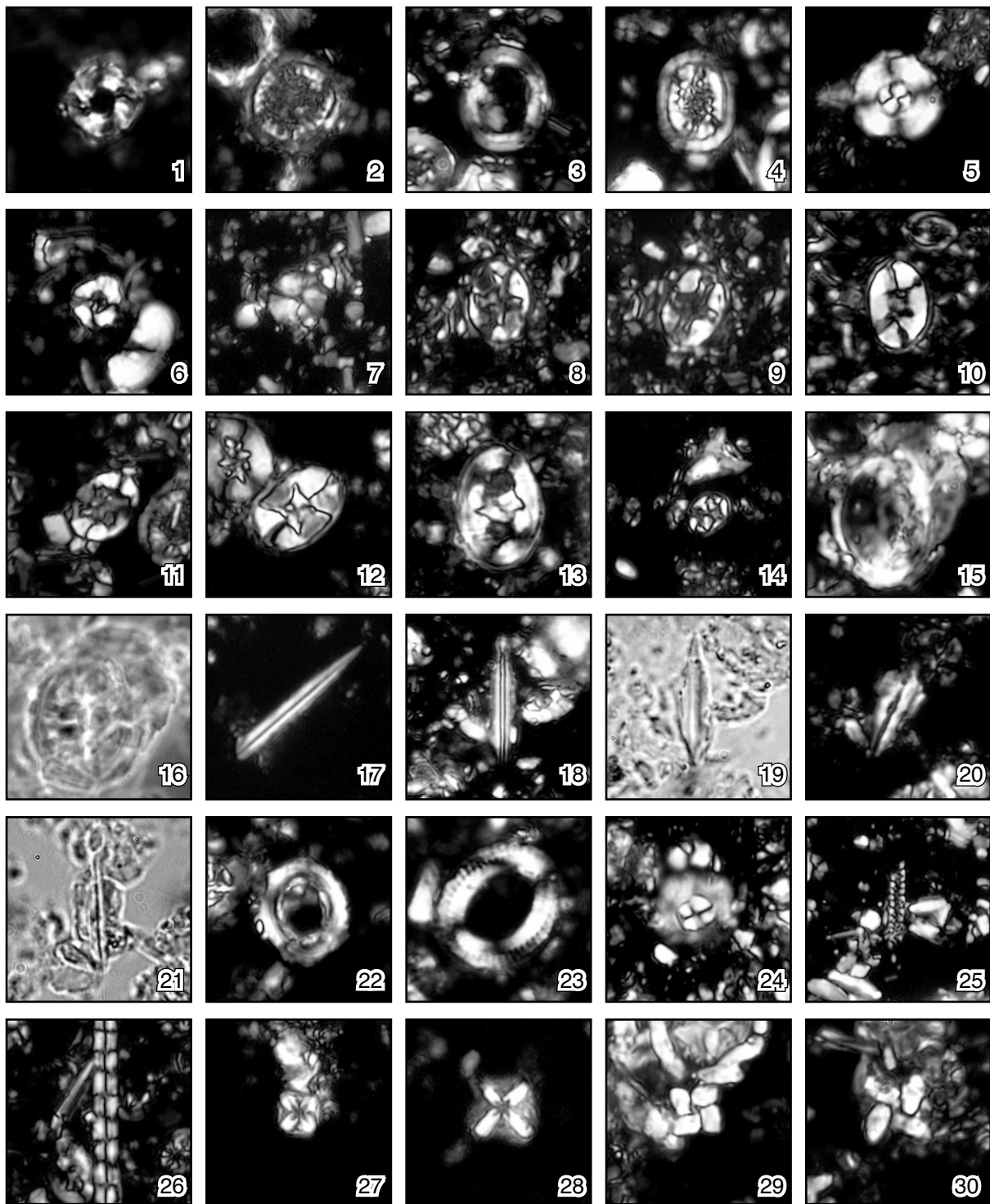
Definition. Interval from the LO of *Lithraphidites quadratus s. s.* to the LO of *L. praequadratus s. s.* and *Cribrocorona gallica*.

Age. Middle Late Maastrichtian.

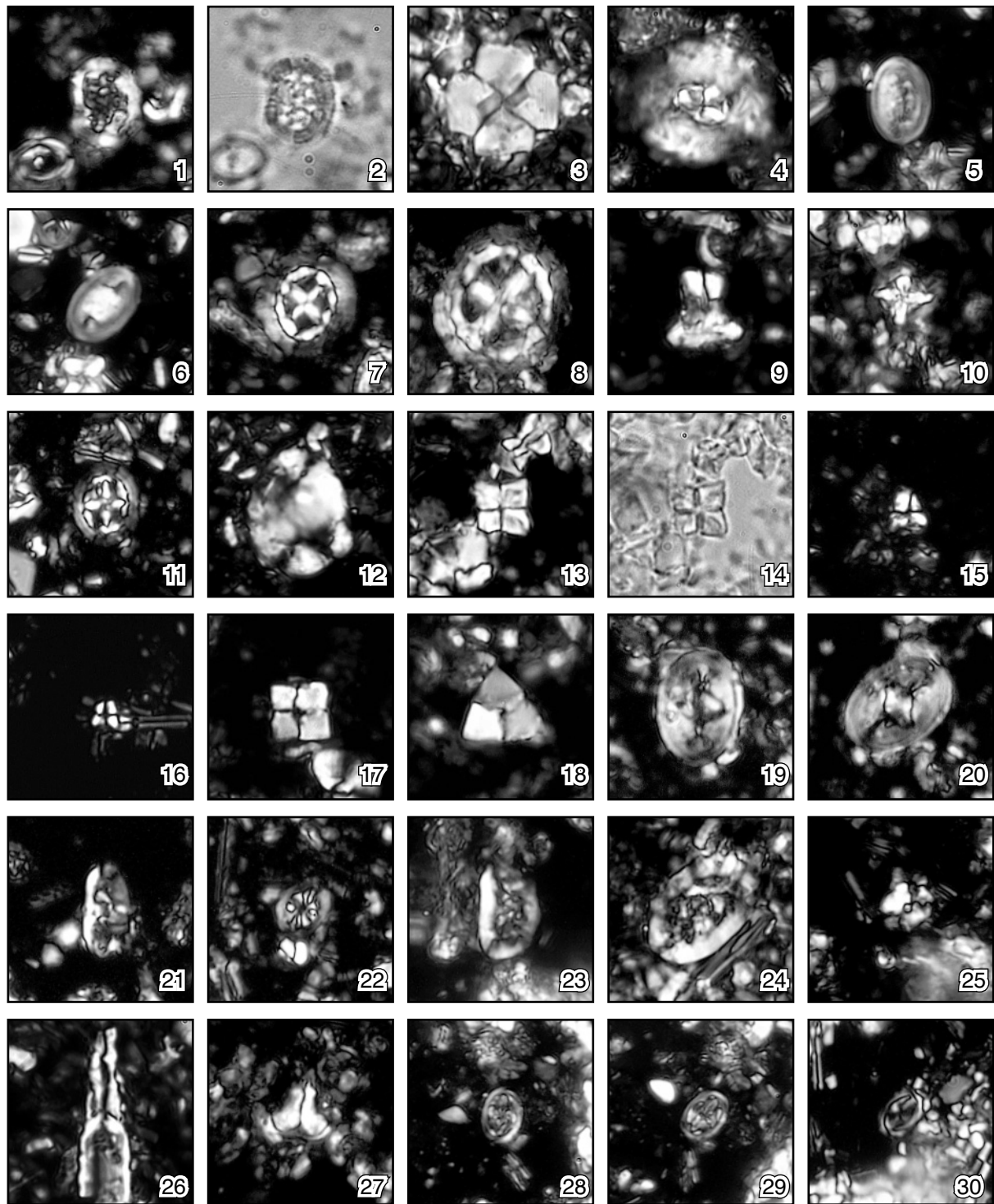
Remarks. The HO of *Petrarhabdus vietus* occurs at about the same level as the LO of *L. praequadratus* and *C. gallica*. The HO of *Ahmuellerella octoradiata* is within KCN3. *C. gallica*



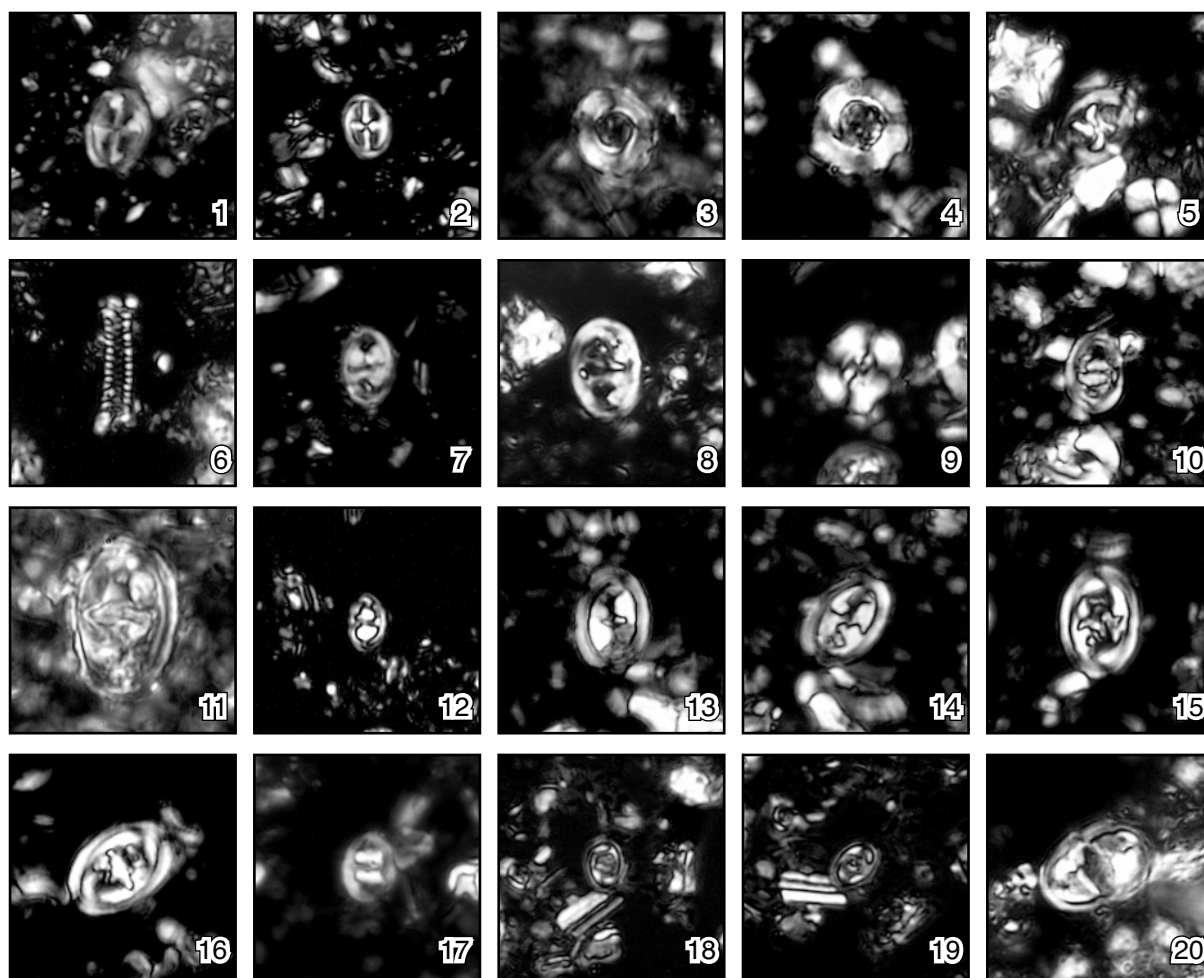
Explanation of Plate 1. All figures taken with cross-polarized light. Scale bar equal to 10 μ m on all figures. **fig. 1.** *Ahmuellerella octoradiata*, ODP 122-761B-23X-5, 120 cm. **fig. 2.** *Ahmuellerella regularis*, ODP 122-762C-47X-3, 22 cm. **fig. 3.** *Angulofenestrellithus snyderi*, ODP 122-761B-24X-1, 110 cm. **fig. 4.** *Arkhangelskiella confusa*, ODP 122-761B-24X-2, 110 cm. **fig. 5.** *Arkhangelskiella cymbiformis*, ODP 122-762C-43X-1, 95 cm. **fig. 6.** *Aspidolithus parvus constrictus*, ODP 122-761B-25X-1 120 cm. **fig. 7.** *Biscutum constans*, Swan ST3, 2240m. **fig. 8.** *Biscutum ellipticum*, ODP 122-762C-46X-3, 116 cm. **fig. 9.** *Biscutum zulloi*, Swan ST3, 2385 m. **fig. 10.** *Braarudosphaera bigelowii*, Kimberley 1, 2280 m. **fig. 11.** *Broinsonia signata*, Swan ST3, 2385m. **figs 12–13.** *Ceratolithoides aculeus*, Swan ST3, 2310 m. **figs 14–15.** *Ceratolithoides arcuatus*, Langhorne 1, 2386.5 m. **figs 16–17.** *Ceratolithoides indiensis*, ODP 122-761B-24X-1, 110 cm. **fig. 18.** *Ceratolithoides kamptneri*, Parry 1, 2209 m. **fig. 19.** *Ceratolithoides kamptneri*, Birch 1, 2057.5 m. **figs 20–21.** *Ceratolithoides quasiarcuratus*, Swan ST3, 2310 m. **figs 22–23.** *Ceratolithoides ultimus*, Swan ST3, 2150 m. **fig. 24.** *Chiastozygus amphipons*, Langhorne 1, 2292.5 m. **fig. 25.** *Chiastozygus antiquus*, Kimberley 1, 2225m. **fig. 26.** *Corollithion completum*, Birch 1, 2057.5 m. **fig. 27.** *Corollithion exiguum*, ODP 122-761B-25X-4, 121 cm. **fig. 28.** *Corollithion madagaskarensis*, Kimberley 1, 2225 m. **fig. 29.** *Cretarhabdus conicus*, Langhorne 1, 2386.5 m. **fig. 30.** *Cretarhabdus multicavus*, Swan ST3, 2310 m.



Explanation of Plate 2. All figures taken with cross-polarized light, except figs 16, 19, 21, which were taken with plain light. Scale bar equal to 10 μ m on all figures. **fig. 1.** *Cribracorona gallica*, ODP 122-762C-43X-1, 96 cm. **fig. 2.** *Cribrosphaerella circula*, Kimberley 1, 2280 m. **fig. 3.** *Cribrosphaerella daniae*, ODP 122-762C-43X-1, 96 cm. **fig. 4.** *Cribrosphaerella ehrenbergii*, ODP 122-761B-24X-2, 110 cm. **fig. 5.** *Cyclagelosphaera reinhardtii*, Swan ST3, 2310 m. **fig. 6.** *Cylindralithus* sp. 2, ODP 122-761B-25X-1, 120 cm. **fig. 7.** *Discorhabdus ignotus*, ODP 761B-25X-1, 120 cm. **figs 8–9.** *Eiffellithus eximius*, Birch 1, 2208 m. **fig. 10.** *Eiffellithus gorkae*, ODP 761B-24X-2, 110 cm. **fig. 11.** *Eiffellithus parallelus*, ODP 762C-43X-1, 95 cm. **fig. 12.** *Eiffellithus turriseiffellii*, OODP 122-23X-5, 120 cm. **fig. 13.** *Gorkaea pseudanthophorus*, Langhorne 1, 2292.5 m. **fig. 14.** *Helicolithus trabeculatus* (small), Swan ST3, 2240 m. **figs 15–16.** *Kamptnerius magnificus*, ODP 122-762C-46X-4, 127 cm. **fig. 17.** *Lithraphidites carniolensis*, Delta 1, 2867.5 m. **figs 18–19.** *Lithraphidites praequadratus*, Birch 1, 2057.5 m. **figs 20–21.** *Lithraphidites quadratus*, Swan ST3, 2200 m. **fig. 22.** *Loxolithus teneraretis*, ODP 122-762C-43X-1, 95 cm. **fig. 23.** *Manivitella pemmatoidea*, ODP 122-761B-24X-2, 110 cm. **fig. 24.** *Markalius inversus*, Parry 1, 2194 m. **fig. 25.** *Microrhabdulus belgicus*, ODP 122-761B, 25X-1, 120 cm. **fig. 26.** *Microrhabdulus decoratus*, ODP 761B-25X-1, 120 cm. **fig. 27.** *Micula cubiformis*, Swan ST3, 2300 m. **fig. 28.** *Micula decussata*, Birch 1, 2057.5 m. **fig. 29.** *Micula murus*, ODP 122-762C-43X-1, 95 cm. **fig. 30.** *Micula prinsii*, ODP 122-762C-43X-1, 95 cm.



Explanation of Plate 3. All figures taken with cross-polarized light, except figs 2 and 14 which were taken with plain light. Scale bar equal to 10 μ m on all figures. **figs 1–2.** *Nephrolithus frequens*, ODP 762C-43X-1, 95 cm. **fig. 3.** *Petrarhabdus copulatus*, ODP 761B-25X-4, 121 cm. **fig. 4.** *Petrarhabdus vietus*, Swan ST3, 2310 m. **figs 5–6.** *Podorhabdus? elkefensis*, Langhorne 1, 2292.5 m. **fig. 7.** *Prediscosphaera cretacea*, ODP 762C-47X-1, 107 cm. **fig. 8.** *Prediscosphaera grandis*, Swan ST3, 2150 m. **fig. 9.** *Prediscosphaera majungae*, ODP 761B-21X-4, 144 cm. **fig. 10.** *Prediscosphaera majungae*, ODP 762C-43X-1, 95 cm. **fig. 11.** *Prediscosphaera spinosa*, ODP 762C-47X-1, 107 cm. **fig. 12.** *Prolatipatella mutilcarinata*, Swan ST3, 2150 m. **figs 13–14.** *Pseudomicula quadrata*, ODP 762C-43X-4, 46 cm. **fig. 15.** *Quadrum bengalensis*, Rothbury 1, 2503 m. **fig. 16.** *Quadrum bengalensis*, ODP 761B-21X-4, 144 cm. **fig. 17.** *Quadrum gothicum*, ODP 761B-25X-1, 120 cm. **fig. 18.** *Quadrum trifidum*, ODP 761B-25X-1, 120 cm. **figs 19–20.** *Reinhardtites levis*, ODP 761B-25X-1, 120 cm. **fig. 21.** *Rhagodiscus angustus*, Delta 1, 2867.5 m. **fig. 22.** *Rhagodiscus plebius*, ODP 762C-47X-1, 107 cm. **fig. 23.** *Rhagodiscus plebius*, Delta 1, 2875 m. **fig. 24.** *Rhagodiscus splendens*, ODP 761B-24X-2, 110 cm. **fig. 25.** *Russellia bukryi*, Kimberley 1, 2225 m. **fig. 26.** *Scampanella* sp., ODP 761B-24X-2, 110 cm. **fig. 27.** *Semihololithus priscus*, Langhorne 1, 2292.5 m. **figs 28–29.** *Staurolithites ellipticus*, Langhorne 1, 2292.5 m. **fig. 30.** *Staurolithites laffittei*, ODP 762C-46X-4, 127 cm.



Explanation of Plate 4. All figures taken with cross-polarized light. Scale bar equal to 10 μ m on all figures. **fig. 1.** *Staurolithites mielnicensis*, Langhorne 1, 2354 m. **fig. 2.** *Staurolithites stradneri*, Swan 2150 m. **fig. 3.** *Stoverius coangustatus* n. sp., ODP 761B-24X-2, 110 cm. **fig. 4.** *Stoverius coangustatus* n. sp., ODP 761B-25X-1, 120 cm. **fig. 5.** *Tegumentum stradneri*, ODP 761B-25X-1, 120 cm. **fig. 6.** *Tetrapodorhabdus decorus* spine, Swan ST3, 2240 m. **fig. 7.** *Tranolithus phacelosus*, Rothbury 1, 2640 m. **fig. 8.** *Tranolithus phacelosus*, Delta 1, 2875 m. **fig. 9.** *Watznaueria barnesae*, ODP 762C-43X-1, 95 cm. **fig. 10.** *Zeughrabdotus bicrescenticus*, ODP 761B-25X-1, 120 cm. **fig. 11.** *Zeughrabdotus embergeri*, Rothbury 1, 2503 m. **fig. 12.** *Zeughrabdotus minimus* n. comb., Swan ST3, 2300 m. **figs 13–14.** *Zeughrabdotus praesigmoides*, ODP 761B-25X-1, 120 cm. **figs 15–16.** *Zeughrabdotus spiralis*, ODP 761B-25X-1, 120 cm. **fig. 17.** *Zeughrabdotus tarboulensis*, Langhorne 1, 2292.5m. **figs 18–19.** *Zeughrabdotus trivectis*, Kimberley 1, 2240 m. **fig. 20.** *Zeughrabdotus wynnayi* n. comb., Swan ST3, 2320 m.

has been observed as ranging from the Late Campanian (?) to the Maastrichtian by Perch-Nielsen (1985), and Coniacian to Maastrichtian by Burnett (1998). *Stoverius coangustatus* n. sp. (the HO of which marks the base of Subzone KCN4a) ranges down into the Middle Campanian (unpublished work by RJC), and can look somewhat similar to *C. gallica* (especially when heavily overgrown), which we consider explains longer ranges of *C. gallica* recorded in other studies.

Zone KCN4

Definition. Interval from the LO of *Lithraphidites praequadratus* s. s. and *Cribrocorona gallica* to the HO of *Reinhardtites levis*.

Age. Early Late Maastrichtian.

Remarks. The LO of *L. praequadratus* is not used as a zonal marker in either of the zonations of Sissingh (1977) and Burnett (1998). Burnett (1998, fig. 6.5, p. 152) shows the FO of *L. praequadratus* in the mid-Campanian, much lower than we have found in this study.

Subzone KCN4a

Definition. Interval from the LO of *Lithraphidites praequadratus* s. s. and *Cribrocorona gallica* to the HO of *Stoverius coangustatus* n. sp.

Age. Early Late Maastrichtian.

Subzone KCN4b

Definition. Interval from the HO of *Stoverius coangustatus* n. sp. to the HO of *Zeugrhabdotus bicrescenticus*.

Age. Early Late Maastrichtian.

Remarks. This work confirms the placement of the HO of *Z. bicrescenticus* above the HO of *Reinhardtites levis*, as shown by Network Stratigraphic in Burnett (1998; fig. 6.6) and Bergen in Bergen & Sikora (1999).

Subzone KCN4c

Definition. Interval from the HO of *Zeugrhabdotus bicrescenticus* to the HO of *Reinhardtites levis*.

Age. Earliest Late Maastrichtian.

Zone KCN5

Definition. Interval from the HO of *Reinhardtites levis* to the HO of *Tranolithus phacelosus*.

Age. Late Early Maastrichtian.

Remarks. KCN5 is missing in all of the sections examined in this study, except in Delta-1 and ODP Hole 762C, where short intervals (assigned to KCN5 or 6) above the HO of *Aspidolithus parvus constrictus* contain both *R. levis* and *Z. bicrescenticus*, as well as the planktonic foraminifer *Abathomphalus mayaroensis* (see KPF zonation below), suggesting that *R. levis* and *Z. bicrescenticus* are reworked, or that *A. mayaroensis* is caved or represents sample or laboratory contamination.

Zone KCN6

Definition. Interval from the HO of *Tranolithus phacelosus* to the HO of *Aspidolithus parvus constrictus*.

Age. Middle Early Maastrichtian.

Remarks. KCN6 is missing in all of the sections examined in this study, except for Delta-1 and ODP 762C (see Zone KCN5 above).

Zone KCN7

Definition. Interval from the HO of *Aspidolithus parvus constrictus* to the HO of *Eiffellithus eximius*.

Age. Latest Campanian to early Early Maastrichtian.

Remarks. *A. parvus constrictus* is inconsistent in occurrence in many of the sections examined in this study. It is associated with

Quadrum sissinghi, *Q. trifidum*, and *Q. gothicum*, which are much rarer and inconsistent in their occurrence.

Planktonic foraminiferal biostratigraphy

All taxa referred to in this section are illustrated in Plates 5–8.

Zone KPF1

Definition. Interval from the HO of Cretaceous planktonic foraminifera to the LO of *Racemiguembelina fruticosa*.

Age. Early Late to late Late Maastrichtian.

Remarks. This zone contains a diverse, abundant planktonic foraminiferal fauna dominated by heterohelicids and rugoglobigerinids, including *Heterohelix globulosa*, *Heterohelix planata*, *Heterohelix rajagopalani*, *Laeviheterohelix glabrans*, *Planoglobulina acervulinoides*, *Pseudoguembelina palpebra*, *Pseudotextularia elegans*, and *Rugoglobigerina rugosa*. *Racemiguembelina fruticosa* varies in abundance, but is consistently recorded. Keeled forms are represented by *Abathomphalus mayaroensis*, *Globotruncana arca*, *Globotruncana falsostuarti*, *Globotruncanella petaloidea*, *Globotruncanella angulata*, and *Globotruncanella stuarti*. The LO of *R. fruticosa* predates the LO of *C. contusa*, allowing the zone to be subdivided.

Subzone KPF1a

Definition. Interval from the HO of Cretaceous planktonic foraminifera to the LO of *Contusotruncana contusa*.

Age. Middle to late Late Maastrichtian.

Remarks. *C. contusa* is rare and sporadic in the Vulcan Sub-basin, but occurs more consistently on the Exmouth and Wombat Plateaus. It is more common towards the top of the zone.

Subzone KPF1b

Definition. Interval from the LO of *Contusotruncana contusa* to the LO of *Racemiguembelina fruticosa*.

Age. Middle Late Maastrichtian.

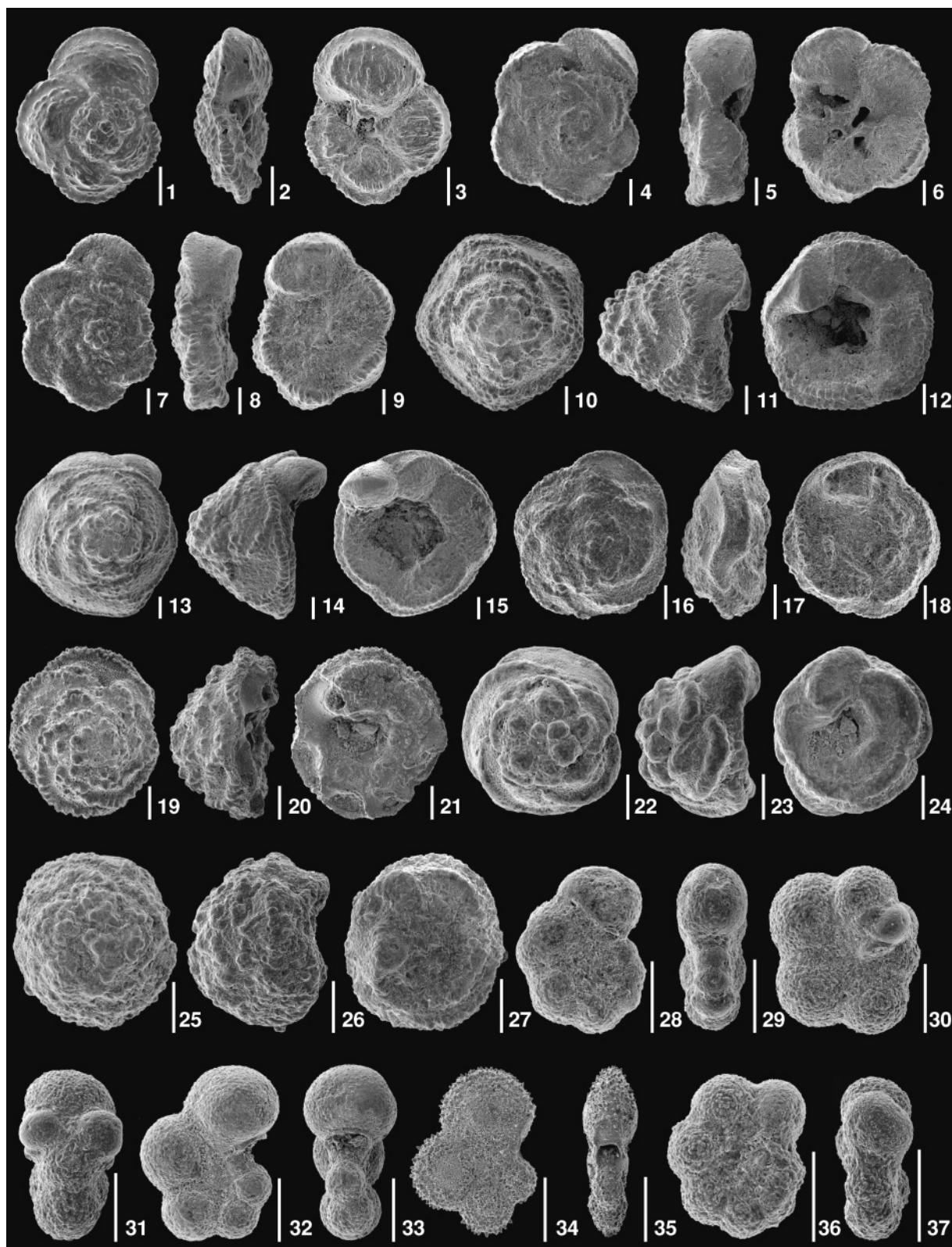
Remarks. A short duration for Subzone KPF1b is indicated by equivalent LOs for *C. contusa* and *R. fruticosa* in about half of the wells examined. It is also possible that a short hiatus is present with KPF1b.

Zone KPF2

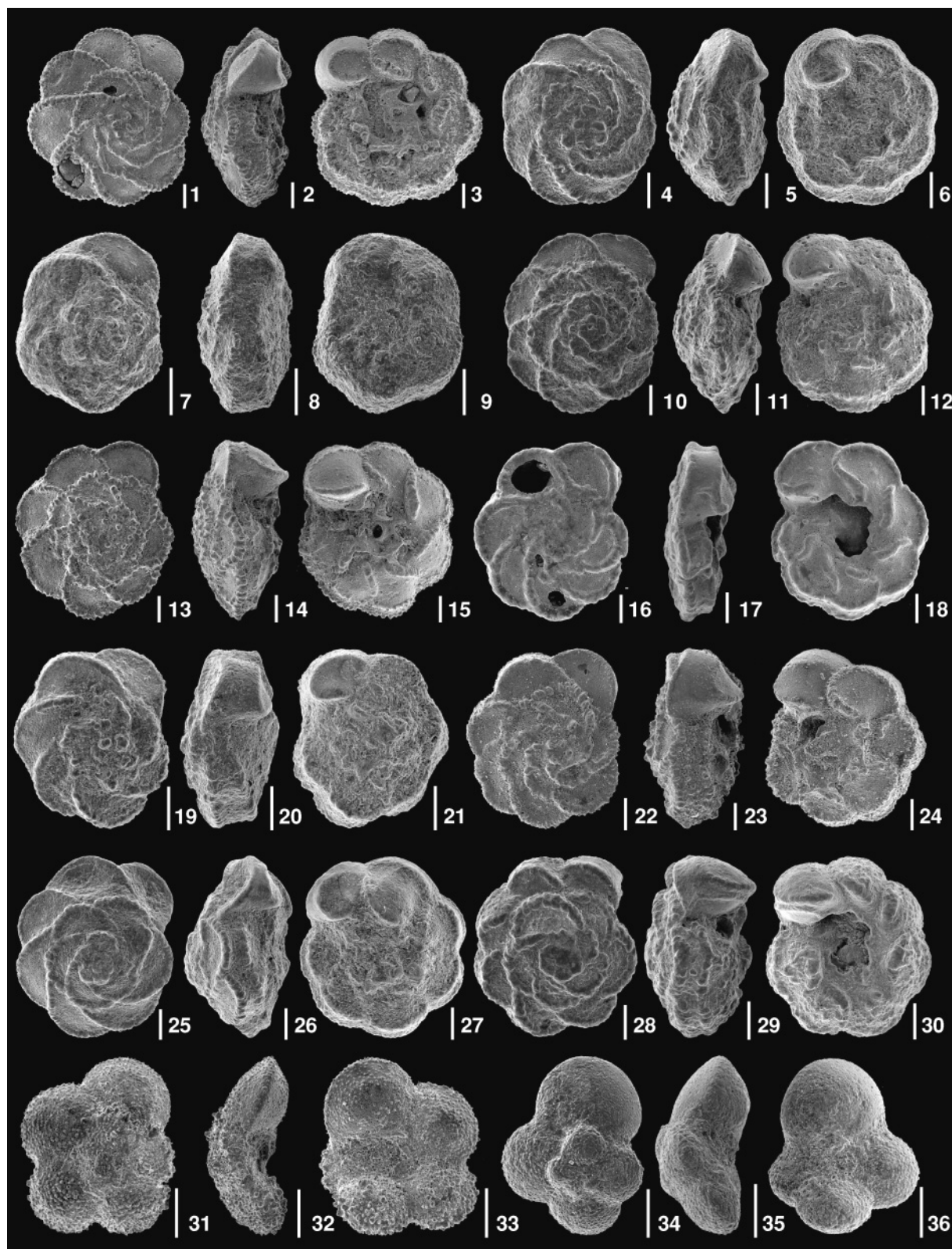
Definition. Interval from the LO of *Racemiguembelina fruticosa* to the LO of *Abathomphalus mayaroensis*.

Age. Early Late Maastrichtian

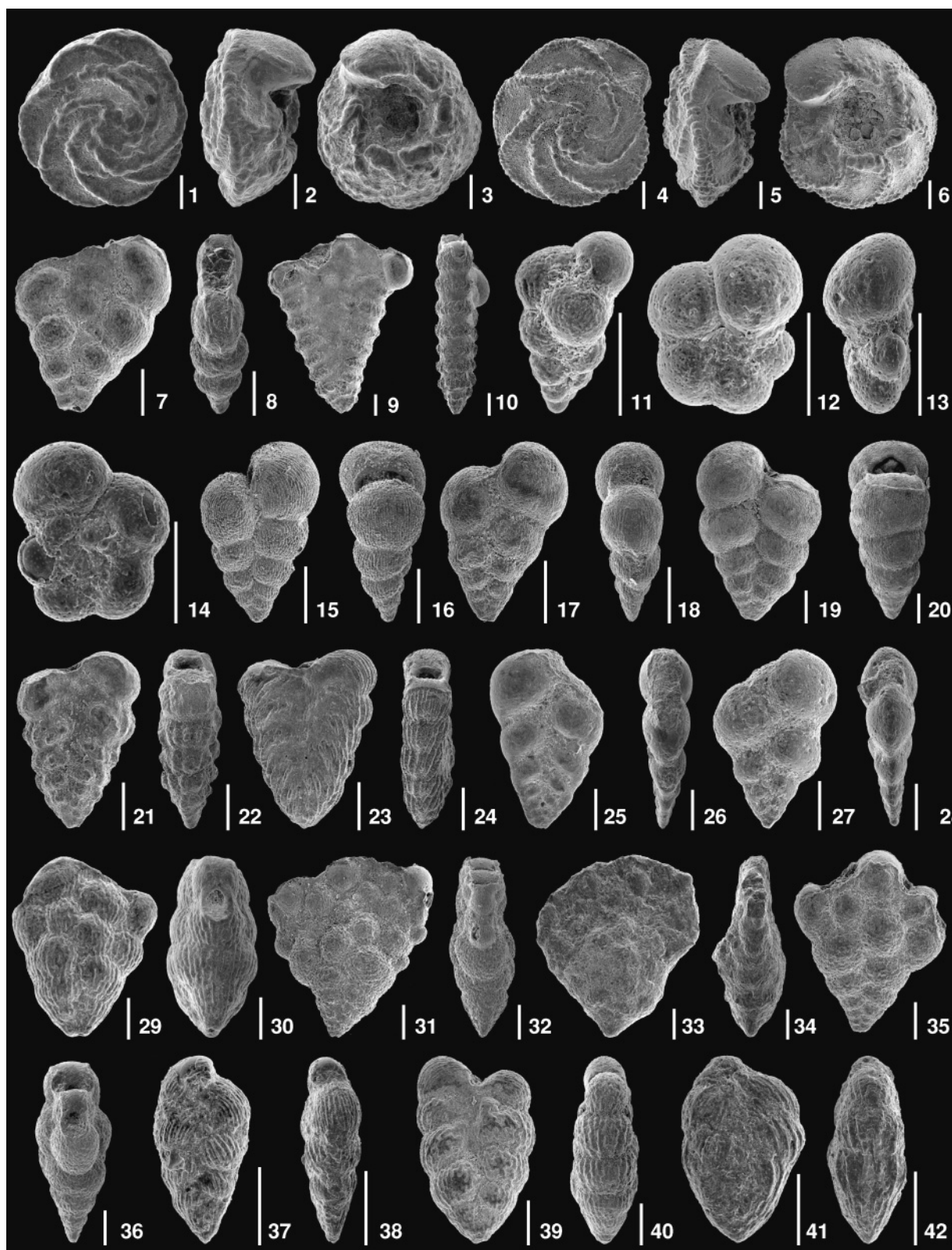
Remarks. *Abathomphalus mayaroensis* is rare and somewhat sporadic near the base of its range in the Vulcan Sub-basin, but



Explanation of Plate 5. All figures SEM (Scanning Electron Microscope) images. Scale bar equal to 0.1 mm on all figures. **figs 1–3.** *Abathomphalus intermedius*, ODP 761B-22X-3, 115 cm. **figs 4–6.** *Abathomphalus mayaroensis*, ODP 761B-23X-5, 5–6 cm. **figs 7–9.** *Abathomphalus mayaroensis*, Parry 1, 2173 m. **figs 10–12.** *Contusotruncana contusa* (angular morphotype), ODP 761B-21X-4, 144–145 cm. **figs 13–15.** *Contusotruncana contusa* (spherical morphotype), ODP 762C-43X-4, 45–46 cm. **figs 16–18.** *Contusotruncana fornicata*, Birch 1, 2208 m. **figs 19–21.** *Contusotruncana* cf. *patelliformis*, ODP 761B-21X-5, 140–141 cm. **figs 22–24.** *Contusotruncana* cf. *plicata*, ODP 761B-21X-4, 144–145 cm. **figs 25–27.** *Contusotruncana walfischensis*, Parry 1, 2178.5 m. **figs 28–29.** *Globigerinelloides* cf. *alvarezi*, Birch 1, 2208 m. **figs 30–31.** *Globigerinelloides multispina*, Swan 3ST, 2150 m. **figs 32–33.** *Globigerinelloides prairiehillensis*, ODP 762C-48X-4, 40–41 cm. **figs 34–35.** *Globigerinelloides subcarinatus*, ODP 761B-24X-2, 110–111 cm. **figs 36–37.** *Globigerinelloides ultramicra*, Leeuw 1, 1639 m.



Explanation of Plate 6. All figures SEM images. Scale bar equal to 0.1 mm on all figures. **figs 1–3.** *Globotruncana arca*, ODP 761B-24X-2, 110–111 cm. **figs 4–6.** *Globotruncana arca*, Parry 1, 2256 m. **figs 7–9.** *Globotruncana bulloides*, Rothbury 1, 2640 m. **figs 10–12.** *Globotruncana dupeublei*, Birch-1, 1987.3 m. **figs 13–15.** *Globotruncana falsostuarti*, ODP 761B-24X-2, 110–111 cm. **figs 16–18.** *Globotruncana linneiana*, ODP 761B-25X-1, 120–122 cm. **figs 19–21.** *Globotruncana linneiana*, Swan 3ST, 2425 m. **figs 22–24.** *Globotruncana* cf. *linneiana*, ODP 761B-24X-2, 110–111 cm. **figs 25–27.** *Globotruncana orientalis*, Parry 1, 2224 m. **figs 28–30.** *Globotruncana* cf. *ventricosa*, ODP 761B-21X-4, 144–145 cm. **figs 31–33.** *Globotruncanella havanensis*, ODP 761B-21X-5, 140–141 cm. **figs 34–36.** *Globotruncanella petaloidea*, Parry 1, 2209 m.



Explanation of Plate 7. All figures SEM images. Scale bar equal to 0.1 mm on all figures. **figs 1–3.** *Globotruncanita angulata*, ODP 761B-21X-4, 144–145 cm. **figs 4–6.** *Globotruncanita stuarti*, ODP 761B-21X-5, 140–141 cm. **figs 7–8.** *Gublerina acuta*, ODP 762C-46X-3, 116–117 cm. **figs 9–10.** *Gublerina cuvillieri*, ODP 761B-24X-2, 110–111 cm. **fig. 11.** *Guembilitria cretacea*, ODP 762C-46X-3, 116–117 cm. **figs 12–14.** *Hedbergella* cf. *holmdelensis*, Birch 1, 2184.8 m. **figs 15–16.** *Heterohelix globulosa*, ODP 761B-22X-5, 106–107 cm. **figs 17–18.** *Heterohelix planata*, ODP 762C-46X-3, 116–117 cm. **figs 19–20.** *Heterohelix* cf. *punctulata*, ODP 761B-25X-2, 105–106 cm. **figs 21–22.** *Heterohelix rajagopalani*, ODP 762C-44X-4, 84–85 cm. **figs 23–24.** *Heterohelix semicostata*, ODP 761B-25X-2, 105–106 cm. **figs 25–26.** *Laeviheterohelix* cf. *dentata*, ODP 762C-47X-5, 106–107 cm. **figs 27–28.** *Laeviheterohelix glabrans*, Parry 1, 2209 m. **figs 29–30.** *Planoglobulina acervulinoides*, ODP 761B-21X-4, 144–145 cm. **figs 31–32.** *Planoglobulina multicamerata*, ODP 761B-24X-2, 110–111 cm. **figs 33–34.** *Planoglobulina multicamerata*, Swan 3ST, 2320 m. **figs 35–36.** *Planoglobulina riograndensis*, ODP 762C-46X-3, 116–117 cm. **figs 37–38.** *Pseudoguembelina costulata*, Swan 3ST, 2310 m. **figs 39–40.** *Pseudoguembelina palpebra*, ODP 762C-44X-6, 66–67 cm. **figs 41–42.** *Pseudoguembelina excolata*, Swan 3ST, 2320 m.

is more common and consistent on the Exmouth and Wombat Plateaus. In this study, the LO of *A. mayaroensis* is found at consistently lower levels than the LOs of *R. fructicosa* and *C. contusa*. This contrasts with previous northwestern margin zonations (Wright & Apthorpe, 1976; Wonders, 1992; Zepeda, 1998; and the original KPF zonation), and with the Tethyan zonation of Robaszynski & Caron (1995). These studies record the LOs of *C. contusa* and *R. fructicosa* below the LO of *A. mayaroensis*. Planktonic foraminiferal abundance and diversity remains high within this zone, and most species found in KPF1 are represented.

Subzone KPF2a

Definition. Interval from the LO of *Racemiguembelina fructicosa* to the LO of *Racemiguembelina powelli*.

Age. Early Late Maastrichtian.

Remarks. Differentiation of *R. fructicosa* and *R. powelli* follows the taxonomy of Smith & Pessagno (1973) and Nederbragt (1991), whereby *R. fructicosa* has four to five sets of multiserial chambers, and *R. powelli* has one to two sets of multiserial chambers. These forms are part of a lineage in which *R. fructicosa* and *Pseudotextularia intermedia* are end members.

Subzone KPF2b

Definition. Interval from the LO of *Racemiguembelina powelli* to the LO of *Pseudotextularia intermedia*.

Age. Early Late Maastrichtian

Remarks. *Pseudotextularia intermedia* is ancestral to *R. powelli* from which it differs by having only one pair of multiserial chambers, not connected by bridges, on the final chamber. An additional event within this subzone is the HO of the benthonic species *Stensioeina pommerana*.

Subzone KPF2c

Definition. Interval from the LO of *Pseudotextularia intermedia* to the LO of *Abathomphalus mayaroensis*.

Age. Early Late Maastrichtian

Remarks. A number of taxa appear to share a similar LO with *A. mayaroensis*. These species include *Globotruncanita stuarti*, *Globotruncanita angulata*, *Planoglobulina acervulinoides*, and *Pseudoguembelina palpebra*. In this study, the benthonic species *Bolivinoidea draco* and *Bolivinoidea giganteus* were not recorded below this level.

Zone KPF3

Definition. Interval from the LO of *Abathomphalus mayaroensis* to the HO of *Globotruncana linneiana*.

Age. Middle Early to earliest Late Maastrichtian.

Remarks. The planktonic foraminiferal diversity and abundance declines within this zone. Commonly recorded species include *Rugoglobigerina rugosa*, *Heterohelix planata*, *Heterohelix rajagopalani*, *Laeviheterohelix glabrans*, *Guembelitria cretacea*, and *Globigerinelloides prairiehillensis*. Keeled forms are less abundant than in the overlying zones. A reasonably strict taxonomic concept for *Globotruncana linneiana* was maintained throughout this study. Forms assigned to this species are flat and rectangular in profile, with a pair of broadly spaced parallel keels. Other forms which had a low trochospire, were slightly convex on the spiral side, and had a slightly tilted keel band were assigned to *Globotruncana* sp. cf. *G. linneiana*. These morphotypes ranged higher in the study area, and were recorded from beds assigned to Zone KPF1a. The benthonic species *Stensioeina pommerana* is most frequently recorded within this zone, and *Bolivinoidea miliaris* is occasionally present.

Zone KPF4

Definition. Interval from the HO of *Globotruncana linneiana* to the LO of *Gublerina cuvillieri*.

Age. Middle Early Maastrichtian.

Remarks. The HO of *Globotruncana bulloides* is associated with the HO of *G. linneiana*. *Gublerina cuvillieri* is particularly rare and sporadic in the Vulcan Sub-basin, and often it is not possible to differentiate this zone from the older Zone KPF5. Planktonic foraminiferal diversity is lower in comparison to Zones KPF1 and KPF2, and species include *Rugoglobigerina* spp., *Heterohelix* spp., *Globotruncana arca*, *Globigerinelloides* spp. and *Laeviheterohelix glabrans*. *Abathomphalus intermedius*, ancestral to *A. mayaroensis*, is present, mainly in ODP Sites 761B and 762C. The benthonic species *Bolivinoidea delicatulus* is consistently recorded from Zones KPF4 and KPF5.

Zone KPF5

Definition. Interval from the LO of *Gublerina cuvillieri* to the HO of *Heterohelix semicostata*.

Age. Latest Campanian to early Early Maastrichtian.

Zone KPF6

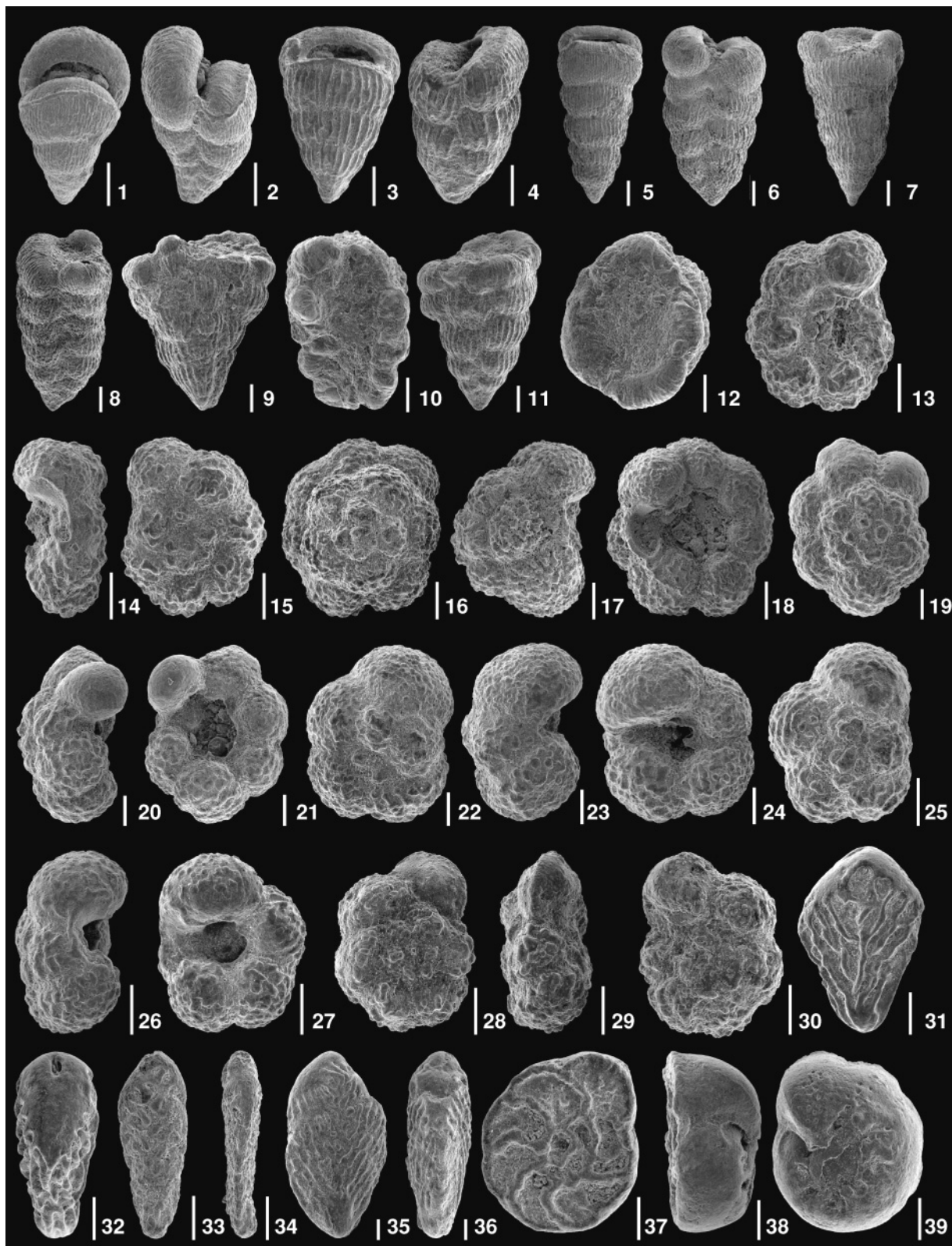
Definition. Total range of *Heterohelix semicostata*.

Age. Late Late Campanian.

Remarks. This zone was only recorded in ODP-762C, and was beyond the initial scope of this study. The LO of *Heterohelix rajagopalani* is possibly coincident with that of *H. semicostata*, and *G. linneiana* is abundant.

Benthonic foraminiferal biostratigraphy

Key taxa referred to in this section are illustrated in Plate 8, figs 31–39.



Explanation of Plate 8. All figures SEM images. Scale bar equal to 0.1 mm on all figures. **figs 1–2.** *Pseudotextularia cushmani*, ODP 761B-25X-2, 105–106 cm. **figs 3–4.** *Pseudotextularia elegans* (coarsely costate morphotype), ODP 762C-43X-4, 45–46 cm. **figs 5–6.** *Pseudotextularia elegans* (moderately costate morphotype), ODP 761B-24X-1, 110–111 cm. **figs 7–8.** *Pseudotextularia intermedia*, ODP 761B-24X-1, 110–111 cm. **figs 9–10.** *Racemiguembelina fruticosa*, Birch 1, 2090.3 m. **figs 11–12.** *Racemiguembelina powelli*, Birch 1, 2090.3 m. **figs 13–15.** *Rugoglobigerina hexacamerata*, ODP 762C-44X-6, 66–67 cm. **figs 16–18.** *Rugoglobigerina milamensis*, ODP 761B-23X-5, 5–6 cm. **figs 19–21.** *Rugoglobigerina pennyi*, ODP 762C-46X-3, 116–117 cm. **figs 22–24.** *Rugoglobigerina rotundata*, ODP 762C-43X-1, 95–96 cm. **figs 25–27.** *Rugoglobigerina rugosa*, ODP 761B-24X-3, 95–96 cm. **figs 28–30.** *Rugotruncana subcircumnodifer*, Parry 1, 2178.5 m. **figs 31–32.** *Bolivinoidea draco*, ODP 762C-44X-6, 66–67 cm. **figs 33–34.** *Bolivinoidea delicatulus*, ODP 762C-44X-1, 85–86 cm. **figs 35–36.** *Bolivinoidea giganteus*, Birch 1, 2048 m. **figs 37–39.** *Stensioeina pommerana*, ODP 762C-47X-5, 106–107 cm.

Zone KBF1

Definition. Total range of *Bolivinoidea draco*.

Age. Middle Early to Late Maastrichtian.

Remarks. The LO of *Bolivinoidea draco* occurs below the HO of *Globotruncana linneiana* (Rexilius, pers. comm., 2001). However, *B. draco* was not recorded below KPF2 in this study, possibly reflecting deeper water conditions.

Integrated calcareous microfossil zonation

Zone KCCM1

Definition. Interval from the HO of Cretaceous planktonic foraminifera to the LO of *Ceratolithoides kamptneri*.

Age. Late Late Maastrichtian.

Subzone KCCM1a

Definition. Interval from the HO of Cretaceous planktonic foraminifera to the LO of *Micula prinsii*.

Age. Latest Maastrichtian.

Subzone KCCM1b

Definition. Interval from the LO of *Micula prinsii* to the LO of *Ceratolithoides kamptneri*.

Age. Late Late Maastrichtian.

Zone KCCM2

Definition. Interval from the LO of *Ceratolithoides kamptneri* to the LO of *Lithraphidites quadratus*.

Age. Middle Late Maastrichtian.

Subzone KCCM2a

Definition. Interval from the LO of *Ceratolithoides kamptneri* to the LO of *Micula murus*.

Age. Middle Late Maastrichtian.

Subzone KCCM2b

Definition. Interval from the LO of *Micula murus* to the LO of *Lithraphidites quadratus s. s.*

Age. Middle Late Maastrichtian.

Zone KCCM3

Definition. Interval from the LO of *Lithraphidites quadratus s. s.* to the LO of *Contusotruncana contusa*.

Age. Middle Late Maastrichtian.

Zone KCCM4

Definition. Interval from the LO of *Contusotruncana contusa* to the LO of *Racemiguembelina fructicosa*.

Age. Middle Late Maastrichtian.

Zone KCCM5

Definition. Interval from the LO of *Racemiguembelina fructicosa* to the LOs of *Lithraphidites praequadratus s. s.* and *Cribracorona gallica*.

Age. Middle Late Maastrichtian.

Zone KCCM6

Definition. Interval from the LOs of *Lithraphidites praequadratus s. s.* and *Cribracorona gallica* to the HO of *Reinhardtites levis*.

Age. Early Late Maastrichtian.

Subzone KCCM6a

Definition. Interval from the LOs of *Lithraphidites praequadratus s. s.* and *Cribracorona gallica* to the HO of *Stoverius coangustatus n. sp.*

Age. Early Late Maastrichtian.

Subzone KCCM6b

Definition. Interval from the HO of *Stoverius coangustatus n. sp.* to the LO of *Racemiguembelina powelli*.

Age. Early Late Maastrichtian.

Subzone KCCM6c

Definition. Interval from the LO of *Racemiguembelina powelli* to the LO of *Pseudotextularia intermedia*.

Age. Early Late Maastrichtian.

Subzone KCCM6d

Definition. Interval from the LO of *Pseudotextularia intermedia* to the LO of *Abathomphalus mayaroensis*.

Age. Early Late Maastrichtian.

Subzone KCCM6e

Definition. Interval from the LO of *Abathomphalus mayaroensis* to the HO of *Zeughradotus bicrescenticus*.

Age. Early Late Maastrichtian.

Subzone KCCM6f

Definition. Interval from the HO of *Zeugrhabdotus bicrescenticus* to the HO of *Reinhardtites levis*.

Age. Earliest Late Maastrichtian.

Zone KCCM7

Definition. Interval from the HO of *Reinhardtites levis* to the HOs of *Tranolithus phacelosus* and *Quadrum tridum*.

Age. Late Early Maastrichtian.

Zone KCCM8

Definition. Interval from the HOs of *Tranolithus phacelosus* and *Quadrum tridum* to the HO of *Globotruncana linneiana*.

Age. Middle Early Maastrichtian.

Subzone KCCM8a

Definition. Interval from the HO of *Tranolithus phacelosus* and *Quadrum tridum* to the HO of *Aspidolithus parvus constrictus*.

Age. Middle Early Maastrichtian.

Subzone KCCM8b

Definition. Interval from the HO of *Aspidolithus parvus constrictus* to the HO of *Globotruncana linneiana*.

Age. Middle Early Maastrichtian.

DISCUSSION

Late Campanian–early Late Maastrichtian disconformity

Our results indicate a significant Late Campanian–early Late Maastrichtian disconformity/hiatus/condensed section, which, at its greatest duration, is between KCCM6 and KCCM11 (see Fig. 6). This event is most easily recognized by the HOs of *Reinhardtites levis* and *Aspidolithus parvus constrictus* which generally last co-occur within the same sample, closely above which the LOs of *Abathomphalus mayaroensis* and *Lithraphidites praequadratus* generally occur. This is the same event as the unconformity between the Campanian Korojon Calcarenite and Upper Maastrichtian Miria Marl in the Southern Carnarvon Basin, and the Campanian Lancelin Beds and the Upper Maastrichtian Breton Marl in the Perth Basin (Shafik, 1993). The mid-Maastrichtian disconformity within the Lancelin-1 Borehole in the Perth Basin, discussed by McNamara *et al.* (1988), would seem to be placed too high in the section, between the LOs of *Lithraphidites quadratus* and *Lithraphidites praequadratus*, whereas it should have been placed between the LO of *L. praequadratus* and the HOs of *Reinhardtites levis* and *Aspidolithus parvus constrictus*. The disconformity correlates to

an interval of short-term sea-level fall during the Early Maastrichtian (Haq *et al.*, 1987), however we do not regard sea-level fall as the direct cause of the disconformity, as the wells examined in this study were under bathyal (>500 m) water-depths during the latest Campanian and Late Maastrichtian.

Shafik (1998) discussed ODP Holes 761B and 762C, and reinterpreted the calcareous nannofossil data of Bralower & Siesser (1992) and the planktonic foraminiferal data of Wonders (1992). Shafik recognized the same disconformity as we do in Hole 762C, but not in Hole 761B. Golovchenko *et al.* (1992) discuss sedimentary cycles in Holes 761B and 762C, and interpret an upper Maastrichtian nondepositional event at *c.* 67 Ma, although this timing must be regarded as suspect, because none of the biostratigraphic or palaeomagnetic investigations in von Rad *et al.* (1992) recognized the presence of any Maastrichtian disconformity. Apthorpe (1979) suggested that a ‘mid-Maastrichtian’ disconformity (=Early Maastrichtian using the time-scale of Gradstein *et al.*, 1994) is widespread on the western Australian margin, as she was unable to recognize Zone C12 (of mid-Maastrichtian age) in 45 of the 52 wells she studied.

The presence of the disconformity is uncertain in the Vulcan Sub-basin, where sampling gaps in the wells we examined are larger than in the ODP wells from the Exmouth Plateau, and where both nannofossils and foraminifera have significantly poorer preservation and lower abundances. Within the limits of sampling and sporadic fossil occurrences, the biostratigraphic sequence in the Vulcan Sub-basin wells is broadly similar to that of the ODP wells, suggesting that a disconformity in hemipelagic sediment between turbidite sands, or a condensed hemipelagic sequence between turbidite sands, may be present.

Isotopic and palaeoecological evidence suggests that a major reorganisation in ocean circulation patterns occurred near the Early–Late Maastrichtian boundary (Barrera, 1994; MacLeod, 1994b; Huber *et al.*, 1995; MacLeod & Huber, 1996; Barrera *et al.*, 1997; Frank & Arthur, 1999). Prior to reorganization, Cretaceous oceans had been characterized by relatively high temperatures, high sea-level, and a low-latitudinal temperature gradient (MacLeod, 1994b). High rates of evaporation at low latitudes and high temperatures at high latitudes resulted in sluggish, saline, low-oxygen bottom-water (MacLeod, 1994b). A gradual cooling trend in the Late Campanian and Early Maastrichtian intensified high-latitude formation of cold, oxygenated, bottom-waters and increased latitudinal temperature-gradients (Barrera, 1994; MacLeod & Huber, 1996; Barrera *et al.*, 1997). During this time, the Southern and Indian Oceans were isolated by geographical barriers between Antarctica and South America and in the central Atlantic, which inhibited the free circulation of intermediate to deep waters. As a result bottom-waters generated around Antarctica would have flowed north past the northwestern Australian margin into the Tethys Ocean. If these bottom waters were corrosive or if current strengths were high enough this could explain the widespread Early Maastrichtian hiatus found on the Western Australian margin. Near the Early–Late Maastrichtian boundary the geographical barrier formed by the Rio Grande Rise and Walvis Ridge in the Atlantic Ocean was breached by sea-floor spreading on the Mid-Atlantic Ridge, allowing freer circulation of bottom-waters between the North Atlantic and Indian Oceans (Frank & Arthur, 1999).

Calcareous nannofossils

Species commonly found in the material examined in this study include *Arkhangelskiella* spp., *Cribrosphaerella ehrenbergii* (which is abundant in almost all samples examined), *Eiffellithus turriseiffelii* (with less common *E. parallelus* and *E. gorkae*), *Lithraphidites carniolensis* (with much less common *L. quadratus* and *L. praequadratus*), *Micula decussata* (with less common *M. cubiformis*), *Prediscosphaera cretacea* (which is also abundant in almost all samples examined, with less common *P. spinosa*, *P. majungae* and rare *P. grandis*), *Retecapsa* spp., *Watznaueria barnesae* and *Zeugrhabdotus spiralis*. Nannofossil abundance was generally high to very high in the ODP holes, and low to moderate in the wells from the Vulcan Sub-basin. Many of the turbidite sands in the Vulcan Sub-basin are barren of nannofossils. Nannofossil preservation was generally moderate to good, particularly in the ODP holes.

In all of the sections examined *Micula murus* and *M. prinsii* are very rare and sporadic. These species are interpreted to have Tethyan affinities (Thierstein, 1981; Henriksson, 1993), so the study area is probably close to the southern limit of their distribution. Therefore, the absence of these species above the LO of *Lithraphidites quadratus* should not be taken to mean that Subzones KCN1a and 1b are definitely not present. The distinction between *L. praequadratus* and *L. quadratus*, following the morphometric criteria of Roth (1978), see Figure 7, is critical in separating Zones KCN2 and 3.

Petrarhabdus vietus is found to have a HO at the same level as the LO of *Lithraphidites praequadratus*. Exactly when, and how, the transition from *P. copulatus* to *P. vietus* occurred is unknown, as *P. copulatus* is present only below the uppermost Campanian–Lower Maastrichtian disconformity. *Podorhabdus? elkefensis* is a little-recorded species which ranges throughout the interval examined in this study. It is not present in ODP Holes 761B and 762C, and is rare and sporadic in occurrence in all of the other sections examined. This suggests that this species prefers more proximal environments, with higher siliciclastic sediment input.

Ceratolithoides aculeus is consistently present in moderate abundances in the Upper Campanian below the unconformity, is rare and sporadic in KCN3 and 4, and very rare in KCN 1 and 2, suggesting an upward cooling trend, as *C. aculeus* is well known to have Tethyan affinities (Burnett, 1997a). *C. indiensis* is rarer and more sporadic in its occurrence than *C. aculeus*, and is very rare above KCN3. It is much more common in ODP Hole 761B than Hole 762C, suggesting that this species is also Tethyan in affinity. In the wells examined from the Vulcan Sub-basin, *C. indiensis* is the most common species of *Ceratolithoides* after *C. aculeus*, but is still rare and sporadic in occurrence. This might suggest that it preferred more distal environments, but equally its occurrence could be due to the generally much lower abundances and poorer preservation of the Vulcan Sub-basin wells compared to the ODP holes. *Quadrum trifidum*, *Q. sissinghii*, and *Q. gothicum* are known to have Tethyan distributions (Thierstein, 1981), and all have very rare and sporadic occurrences in this study, suggesting that the northwestern Australian margin was near the southern limit of their distribution during the latest Campanian.

AUSTRAL PROVINCE		POLARITY	STAGE	TETHYAN PROVINCE	
Event	Zone			Zone	Event
▲ <i>A. mayaroensis</i>	<i>A. mayaroensis</i>	29r	MAASTRICHTIAN	<i>A. mayaroensis</i>	▲ <i>A. mayaroensis</i>
		30n			
		30r			
		31n			
	<i>G. havan.</i>	31r		<i>G. gansseri</i>	
		32n1			

Fig. 8. Comparison of the lowest occurrence of *Abathomphalus mayaroensis* in the high-latitude Austral Province (from Huber, 1990), and the low-latitude Tethyan Province (from Premoli Silva & Sliter, 1994).

Planktonic foraminifera

In Tethyan biostratigraphic schemes, the LO of *Contusotruncana contusa* predates the LO of *Abathomphalus mayaroensis* and defines the *C. contusa* Zone (Dalbiez, 1955; Pessagno, 1967; Van Hinte, 1976; Wonders, 1980; Premoli Silva & Sliter, 1994; Robaszynski & Caron, 1995). Similarly, the LO of *Racemiguembelina fruticosa* occurs below the LO of *A. mayaroensis*, at about the same level as the LO of *C. contusa* (Sigal, 1977; Nederbragt, 1991; Premoli Silva & Sliter, 1994). The results of this study of the Exmouth Plateau and the Vulcan Sub-basin indicate a different sequence of events, with the LOs of *C. contusa* and *R. fruticosa* consistently postdating the LO of *Abathomphalus mayaroensis*. In addition, *Gansserina gansseri*, the LO of which defines the base of a zone in the Tethyan Realm (see Sigal, 1977; Robaszynski & Caron, 1995), is absent from the sections examined in this study.

This contrast between the ranges of *C. contusa*, *R. fruticosa*, *A. mayaroensis* and *G. gansseri* is palaeobiogeographically driven, with the northwestern Australian margin lying in a transitional setting between the Tethyan and Austral Realms. The LO of *A. mayaroensis* has been shown to be a diachronous event, with the species originating at high latitudes (Austral Realm) near the Early–Late Maastrichtian boundary and then migrating equator-ward (Huber 1990, 1991, 1992; Nederbragt, 1998; Frank & Arthur, 1999). In high southern latitude Austral sites, the LO of *A. mayaroensis* occurs within the middle of magnetic Chron 31R (Huber, 1990, 1991, 1992), whereas in low-latitude Tethyan settings such as Gubbio, Italy (Premoli Silva & Sliter, 1994), and the equatorial Pacific (Boersma, 1981) it first occurs in Chron 31N (Fig. 8).

In contrast to *A. mayaroensis*, which appears to have originated at high latitudes, Tethyan species such as *C. contusa*, *G. gansseri* and *R. fruticosa* are absent from Austral sections (e.g. Huber, 1990, 1991: Kerguelen Plateau and Weddell Sea, Southern Ocean; Webb, 1973: Lord Howe Rise, Tasman Sea;

Hornibrook *et al.*, 1989; New Zealand). The transitional setting of the northwestern Australian margin was likely to be near the palaeolatitudinal limit of some Tethyan species such as *R. fructicosa* and *C. contusa* (see Kucera & Malmgren, 1996), and outside the palaeolatitudinal limit of other Tethyan species such as *G. gansseri*. Of interest is that Chungkham & Jafar (1998) record *G. gansseri* from Ukhrul, northeastern India, estimated to have a palaeolatitude of between 20°S and 30°S during the Maastrichtian. Wonders (1992) suggested that *C. contusa* was an immigrant to the northwestern Australian margin and that its appearance in that area postdates its evolutionary appearance elsewhere. Probably of equal importance to the sequence of events recorded on the margin was the northward migration of *A. mayaroensis* and the resultant earlier LO for this species than in the Tethyan Realm.

Whatever the reason for the difference in the sequence of events, the results of this study call into question the validity of the *C. contusa* Zone recorded by previous workers on the northwestern Australian margin. Both Wonders (1992) and Zepeda (1998) record the *C. contusa* Zone from ODP 762C, but neither record *C. contusa* below *A. mayaroensis*. The assignment of samples to the *C. contusa* Zone is based instead on the LO of *Abathomphalus intermedius*, which was used by these workers as a proxy for *C. contusa*. In a separate study of petroleum wells on the northwestern Australian margin, Wright & Apthorpe (1976) also defined a *C. contusa* Zone, with the LO of *C. contusa* as the base and the LO of *A. mayaroensis* marking the upper boundary of the zone. Apthorpe (1979) later highlighted problems with applying this zone to the region and questioned the validity of the LO of *C. contusa* as an event, or whether the absence of this species below *A. mayaroensis* marked a middle Maastrichtian disconformity. In our study, the LOs of *R. fructicosa* and *C. contusa* predate the LO of *A. mayaroensis* in only two wells, Leeuwin-1 and Rothbury-1, situated in the Vulcan Sub-basin, where *A. mayaroensis* was both rare and sporadic. The samples in these wells which contained *R. fructicosa* and *C. contusa* without *A. mayaroensis* also contained the nannofossil *Lithraphidites praequadratus*, the LO of which is found to postdate the LO of *A. mayaroensis* in all other wells studied in the area. As a result it appears that the *C. contusa* Zone is not valid in the study area.

The contrast between the Tethyan and Transitional Province ranges of *A. mayaroensis* has meant considerable revision to the Late Maastrichtian part of the KPF planktonic foraminiferal zonation. Where previously the base of the KPF1 Zone was identified by the LO of *A. mayaroensis* (Rexilius, unpublished data), it is now defined by the LO of *R. fructicosa*. Similarly, where previously the base of the original KPF2 Zone was identified by the LO of *R. fructicosa*, it is now defined by the stratigraphically older placement for the LO of *A. mayaroensis* (Fig. 6).

CONCLUSIONS

Three biostratigraphic zonations are presented for the latest Campanian–Maastrichtian of the Exmouth Plateau and Vulcan Sub-basin, on the northwestern Australian margin, using planktonic foraminifera and calcareous nannofossils. These zonations are revisions of the unpublished KCN (nannofossils), KPF (planktonic foraminifera), and KCCM (combined nannofossils

and foraminifera) zonations. The northwestern Australian margin clearly lay within a diffuse Transitional Province between the warm Tethyan Province to the north and the cool Austral Province to the south. Species of both foraminifera and nannofossils with Tethyan affinities are present with species with Austral affinities. In the KCN zonation, the use of Tethyan species such as *Micula murus*, *M. prinsii*, and *Ceratolithoides kamptneri* is difficult as these species are often rare and sporadic in their distribution. In the KPF zonation, the use of a *Contusotruncana contusa* Zone or *Racemiguembelina fructicosa* Zone predating the *Abathomphalus mayaroensis* Zone was shown to be invalid in the Transitional setting of the northwestern margin. This is probably due to the equator-ward migration of *A. mayaroensis* from the south resulting in an older LO in comparison to Tethyan sections, and/or a later migration of *C. contusa* and *R. fructicosa* into the area.

Revision of the zonations has highlighted a major disconformity, separating Upper Campanian from lower Upper Maastrichtian strata. This disconformity was largely unnoticed in previous examinations of ODP material from Exmouth Plateau, but was recorded by previous workers on the northwestern Australian margin (e.g. Apthorpe, 1979; Shafik, 1993).

ACKNOWLEDGEMENTS

This project was carried out at the University of Western Australia and was funded as a project of the Virtual Centre of Economic Micropalaeontology and Palynology (VCEMP) by the Australian Geological Survey Organisation (AGSO). We thank Clinton Foster of AGSO for his strong support of the project. David Haig, Marjorie Apthorpe, Barry Taylor, Warwick Crowe and Fiona Burns are thanked for their helpful advice during the project. The curatorial staff of the Ocean Drilling Program at Texas A&M University are thanked for their supply of samples from ODP Holes 761B and 762C. The staff at the Centre for Microscopy and Microanalysis, UWA, are thanked for access to the Scanning Electron Microscope.

APPENDIX A: TAXONOMIC NOTES

(with James A. Bergen, BP America, Houston, TX, USA)

Rotelapillus laffittei (Nöel, 1956) Howe *comb. nov.*

Basionym. *Stephanolithion laffittei* Nöel (1956), p. 318, pl. 2, fig 5, non fig. 6.

Reference. Nöel (1956).

Discussion. Nöel (1973) is frequently cited (e.g. Bown, 1998) as having recombined *Stephanolithion laffittei* Nöel (1956) into *Rotelapillus* Noel (1973). Nöel (1973) does not actually contain such a recombination, so it is made here.

Stoverius coangustatus n. sp. Howe, Bergen & Campbell
(Pl. 4, figs 3, 4).

Derivation of name. Latin – *coangusto*: compress, confine, enclose.

Holotype. Plate 4, fig. 4. Paratype Plate 4, fig. 3.

Type locality. Ocean Drilling Program Hole 761B, on the Exmouth Plateau, offshore of northwestern Australia. The holotype is from sample ODP761B-25X-1, 120 cm, and the paratype is from sample ODP761B-24X-2, 110 cm.

Type level. The holotype belongs to Zone KCN7 of this study, Zone UC16 of Burnett (1998), Subzone CC23a of Sissingh (1977) and is of late Late Campanian age. The paratype belongs to subzones KCN4b and KCCM6c of this study, Zone UC19 of Burnett (1998), Subzone CC25a of Sissingh (1977), and is of early Late Maastrichtian age.

Diagnosis. A circular to subcircular species of *Stoverius* with a small central area spanned by two arcuate bars.

Description (light microscope). A medium-sized (holotype 7.2 µm diameter, paratype 6.7 µm, typical range 5.5–7.5 µm), circular to subcircular protolith constructed of two rim cycles. The broad proximal rim cycle is low and constructed of 24–36 radial elements with convex peripheries. These elements exhibit a first-order grey to white birefringence. The distal rim cycle is high and composed of radial elements, with a smooth periphery. The distal rim cycle exhibits a bright first-order yellow-orange to orange birefringence. The width of the distal rim cycle is variable (c. 5 µm diameter in the holotype), being between 50–95% the width of the proximal rim cycle. A low, narrow wall (c. 1.7 µm wide in the holotype) connects the two rim cycles and can be seen upon proximal focus; it exhibits a first-order white birefringence. The central area is small (c. 2.7 µm wide in the holotype), occupying between one-third to one-fifth of the coccolith diameter or width. Two arcuate bars span the small central opening and are orientated with their convex sides facing each other and are joined near the centre; these bars are faintly birefringent, and are rarely preserved.

Occurrence. This species is restricted to the Middle Campanian to lower Upper Maastrichtian on the Northwest Shelf. It has a well-defined highest occurrence in the lower Upper Maastrichtian, approximately coincident with the lowest occurrence of *Lithraphidites praequadratus*, and a well-defined lowest occurrence in the Middle Campanian, at about the same level as the lowest occurrence of *Ceratolithoides aculeus* (unpublished work by RJC). It is also present in Tunisia and the Campanian–Maastrichtian boundary stratotype near Tercis, France (unpublished work by JAB) and also on the Scotian Shelf, offshore eastern Canada (unpublished work by RWH).

Discussion. This species differs from other species of *Stoverius* in having a smaller central area, and a broader proximal rim cycle. *S. coangustatus* evolved from *S. biarcus* during the middle Campanian through restriction of the central area. *S. coangustatus* is distinguished from *Cylindralithus crassus* by having a central structure and a less birefringent distal rim cycle.

Zeughrabdotus minimus (Bukry, 1969) Howe *comb. nov.*

Basionym. *Zygodiscus minimus* Bukry (1969), p. 61, pl. 35, figs 9–11.

Reference. Bukry (1969).

Discussion. *Zygodiscus* is a Palaeocene and Lower Eocene genus with two cycles of elements in its outer wall (following the terminology of Young *et al.*, 1997), while the Mesozoic genus *Zeughrabdotus* has a single cycle of elements in its outer wall. As *Zygodiscus minimus* is a Late Cretaceous species which appears to have a single cycle of elements in its outer wall, it is recombined into *Zeughrabdotus*.

Zeughrabdotus wynnhayi (Risatti, 1973) Howe *comb. nov.*

Basionym. *Zygodiscus wynnhayi* Risatti (1973), p. 22, pl. pl. 9, figs, 21, 22.

Reference. Risatti (1973).

Discussion. See discussion for *Zeughrabdotus minimus* above.

APPENDIX B: ALPHABETICAL LIST OF SPECIES CONSIDERED IN THIS STUDY

Calcareous nannofossils

References not cited in this paper can be found in Perch-Nielsen (1985) and Bown (1998).

Ahmuellerella octoradiata (Gorka, 1957) Reinhardt (1966)

Ahmuellerella regularis (Gorka, 1957) Reinhardt & Gorka (1967)

Angulofenestrellithus snyderi Bukry (1969)

Arkhangelskiella confusa Burnett (1998b)

Arkhangelskiella cymbiformis Vekshina (1959)

Aspidolithus parvus (Stradner, 1963) Noël (1969) ssp. *constrictus* (Hattner *et al.*, 1980) Perch-Nielsen (1984)

Aspidolithus parvus (Stradner, 1963) Noël (1969) ssp. *parvus* (Stradner, 1963) Noël (1969)

Biscutum constans (Gorka, 1957) Black in Black & Barnes (1959)

Biscutum ellipticum (Gorka, 1957) Grün in Grün & Allemann (1975)

Biscutum zulloi Covington (1994)

Braarudosphaera bigelowii (Gran & Braarud, 1935) Deflandre (1947)

Broinsonia signata (Noël, 1969) Noël (1970)

Calculites obscurus (Deflandre, 1959) Prins & Sissingh in Sissingh (1977)

Ceratolithoides aculeus (Stradner, 1961) Prins & Sissingh in Sissingh (1977)

Ceratolithoides amplexor Burnett (1998a)

Ceratolithoides arcuatus Prins & Sissingh in Sissingh (1977)

Ceratolithoides indiensis Burnett (1998a)

Ceratolithoides kamptneri Bramlette & Martini (1964)

Ceratolithoides pricei Burnett (1998a)

Ceratolithoides prominens Burnett (1998a)

Ceratolithoides quasiarcuatus Burnett (1998a)

Ceratolithoides self-trailae Burnett (1998a)

Ceratolithoides ultimus Burnett (1998a)

Chiastozygus amphipons (Bramlette & Martini, 1964) Gartner (1968)

- Chiastozygus antiquus* (Perch-Nielsen, 1973) Burnett (1998b)
Corolithion completum Perch-Nielsen (1973)
Corolithion exiguum Stradner (1961)
Corolithion madagaskarensis Perch-Nielsen (1973)
Cretarhabdus conicus Bramlette & Martini (1964)
Cretarhabdus multicaus Bukry (1969)
Cribrocorona gallica (Stradner, 1963) Perch-Nielsen (1973)
Cribrosphaerella circula (Risatti, 1973)
Cribrosphaerella daniae Perch-Nielsen (1973)
Cribrosphaerella ehrenbergii (Arkhangelsky, 1912) Deflandre
in Piveteau (1952)
Cyclagelosphaera reinhardtii (Perch-Nielsen, 1968) Romein
(1977)
Cylindralithus sp. 2
Discorhabdus ignotus (Gorka, 1957) Perch-Nielsen (1968)
Eiffellithus eximius (Stover, 1966) Perch-Nielsen (1968)
Eiffellithus gorkae Reinhardt (1965)
Eiffellithus parallelus Perch-Nielsen (1973)
Eiffellithus turriseiffellii (Deflandre in Deflandre & Fert,
1954) Reinhardt (1965)
Gartnerago obliquum (Stradner, 1963) Noël (1970)
Gorkaea pseudanthophorus (Bramlette & Martini, 1964) Varol
& Girgis (1994)
Helicolithus trabeculatus (Gorka, 1957) Verbeek (1977)
Kamptnerius magnificus Deflandre (1959)
Lithraphidites carniolensis Deflandre (1963)
Lithraphidites praequadratus Roth (1978)
Lithraphidites quadratus Bramlette & Martini (1964) *emend.*
Roth (1978)
Loxolithus sp. 1 Bergen in Bralower & Bergen (1998)
Loxolithus sp. 2 Bergen in Bralower & Bergen (1998)
Loxolithus teneraretis (Varol, 1991) Howe in Howe *et al.*
(2000)
Lucianorhabdus cayeuxii Deflandre (1959)
Maniviitella pemmatoidea (Deflandre in Manivit, 1965)
Thierstein (1971)
Markalius inversus (Deflandre in Deflandre & Fert, 1954)
Bramlette & Martini (1964)
Microrhabdulus attenuatus (Deflandre, 1959) Deflandre
(1963)
Microrhabdulus belgicus Haye & Towe (1963)
Microrhabdulus decoratus Deflandre (1959)
Microrhabdulus helicoideus Deflandre (1959)
Micula cubiformis Forchheimer (1972)
Micula decussata Vekshina (1959)
Micula murus (Martini, 1961) Bukry (1973)
Micula praemurus (Bukry, 1973) Stradner & Steinmetz
(1984)
Micula prinsii Perch-Nielsen (1979)
Misceomarginatus pleniporus Wind & Wise in Wise & Wind
(1977)
Nephrolithus corystus Wind (1983)
Nephrolithus frequens Gorka (1957)
Octolithus multiplus (Perch-Nielsen, 1973) Romein (1979)
Pervilithus varius Crux (1981) (= *Scampanella* sp. in end-on
view)
Petrarhabdus copulatus (Deflandre, 1959) Wind & Wise in
Wise (1983)
Petrarhabdus vietus Burnett (1998b)
Petrobrasiella bownii Burnett (1998b)
Podorhabdus? elkefensis Perch-Nielsen (1981)
Prediscosphaera arkhangelskyi (Reinhardt, 1965) Perch-
Nielsen (1984)
Prediscosphaera cretacea (Arkhangelsky, 1912) Gartner
(1968)
Prediscosphaera grandis Perch-Nielsen (1979)
Prediscosphaera majungae Perch-Nielsen (1973)
Prediscosphaera spinosa (Bramlette & Martini, 1964) Gartner
(1968)
Prolatipatella multicarinata Gartner (1968)
Pseudomicula quadrata Perch-Nielsen in Perch-Nielsen *et al.*
(1978)
Psyktosphaera firthii Pospichal & Wise (1990)
Quadrum bengalensis Burnett (1998b)
Quadrum gothicum (Deflandre, 1959) Prins & Perch-Nielsen in
Manivit *et al.* (1977)
Quadrum sissinghii Perch-Nielsen (1984)
Quadrum trifidum (Stradner in Stradner & Papp, 1961) Prins
& Perch-Nielsen in Manivit *et al.* (1977)
Reinhardtites levis Prins & Sissingh in Sissingh (1977)
Retecapsa schizobrachiata (Gartner, 1968) Grün in Grün &
Allemann (1975)
Retecapsa spp.
Rhagodiscus angustus (Stradner, 1963) Reinhardt (1971)
Rhagodiscus plebius Perch-Nielsen (1968)
Rhagodiscus reniformis Perch-Nielsen (1973)
Rhagodiscus splendens (Deflandre, 1953) Verbeek (1977)
Rotelapillus laffittei (Noël, 1956) Howe *comb. nov.*
Rucinolithus hayi Stover (1966)
Rucinolithus sp. 8
Russellia bukryi Risatti (1973)
Scampanella spp.
Scapholithus fossilis Deflandre in Deflandre & Fért (1954)
Semihololithus priscus Perch-Nielsen (1973)
Stauroolithites ellipticus (Gartner, 1968) Lambert (1987)
Stauroolithites imbricatus (Gartner, 1968) Burnett (1998b)
Stauroolithites laffittei Caratini (1963)
Stauroolithites mielnicensis (Gorka, 1957) Perch-Nielsen
(1968)
Stauroolithites stradneri (Rood *et al.*, 1971) Bown (1998)
Stoverius coangustatus n. sp.
Tegumentum stradneri Thierstein in Roth & Thierstein (1972)
Tetrapodorhabdus decorus (Deflandre in Deflandre & Fert,
1954) Wind & Wise in Wise & Wind (1977)
Tranolithus phacelosus Stover (1966)
Watznaueria barnesae (Black, 1959) Perch-Nielsen (1968)
Watznaueria ovata Bukry (1969)
Zeughrabdotus bicrescenticus (Stover, 1966) Burnett in Gale
et al. (1996)
Zeughrabdotus embergeri (Noël, 1958) Perch-Nielsen (1984)
Zeughrabdotus minimus (Bukry, 1969) Howe *comb. nov.*
Zeughrabdotus praesigmoides Burnett (1998b)
Zeughrabdotus spiralis (Bramlette & Martini, 1961) Burnett
(1998b)
Zeughrabdotus tarboulensis (Shafik & Stradner, 1971) Howe
in Howe *et al.* (2000)
Zeughrabdotus cf. trivectis Bergen (1994)
Zeughrabdotus wynnhayi (Risatti, 1973) Howe *comb. nov.*

Planktonic foraminifera

Original generic assignment is quoted in square brackets to allow for quick reference to the original citation within the catalogue of Ellis & Messina (1945 *et seq.*). References not cited in this paper can be found in Ellis & Messina (1945 *et seq.*) and Caron (1985).

- Abathomphalus intermedius* (Bolli, 1951) [*Globotruncana*]
Abathomphalus mayaroensis (Bolli, 1951) [*Globotruncana*]
Contusotruncana contusa (Cushman, 1926) [*Pulvinulina arca* var.]
Contusotruncana fornicata (Plummer, 1931) [*Globotruncana*]
Contusotruncana patelliformis (Gandolfi, 1955) [*Globotruncana contusa* subsp.]
Contusotruncana cf. *plicata* (White, 1928) [*Globotruncana conica* var.]
Contusotruncana walfischensis (Todd, 1970) [*Globotruncana*]
Globigerinelloides cf. *alvarezi* (Eternod Olvera, 1959) [*Planomalina*]
Globigerinelloides multispina (Lalicker, 1948) [*Biglobigerinella*]
Globigerinelloides prairiehillensis Pessagno, 1967
Globigerinelloides subcarinatus (Brönnimann, 1952) [*Globigerinella messinae* subsp.]
Globigerinelloides ultramicra (Subbotina, 1949) [*Globigerinella*]
Globotruncana cf. *aegyptiaca* Nakkady, 1950
Globotruncana arca (Cushman, 1926) [*Pulvinulina*]
Globotruncana bulloides Vogler, 1941 [*Globotruncana linnei* subsp.]
Globotruncana dupeblei Caron, Gonzalez Donoso, Robaszynski, & Wonders, 1984
Globotruncana cf. *esnehensis* Nakkady, 1950 [*Globotruncana arca* var.]
Globotruncana falsostuarti Sigal, 1952
Globotruncana insignis Gandolfi, 1955
Globotruncana linneiana (d'Orbigny), 1839 [*Rosalina*]
Globotruncana orientalis El Naggar, 1966
Globotruncana rugosa (Marie, 1941) [*Rosalinella*]
Globotruncana ventricosa White, 1928 [*Globotruncana canaliculata* var.]
Globotruncanella havanensis (Voorwijk, 1937) [*Globotruncana*]
Globotruncanella petaloidea (Gandolfi, 1955) [*Globotruncana*]
Globotruncanita angulata (Tilev, 1951) [*Globotruncana lugeoni* var.]
Globotruncanita cf. *conica* (White, 1928) [*Globotruncana*]
Globotruncanita cf. *pettersi* (Gandolfi, 1955) [*Globotruncana rosetta* subsp.]
Globotruncanita stuarti (de Lapparent, 1918) [*Rosalina*]
Gublerina acuta De Klasz, 1953
Gublerina cuvillieri Kikoin, 1948
Guembilitria cretacea Cushman, 1933
Hedbergella cf. *holmdeleensis* Olsson, 1964
Heterohelix globulosa (Ehrenberg, 1840) [*Textularia*]
Heterohelix planata (Cushman, 1938) [*Guembelina*]
Heterohelix cf. *punctulata* (Cushman, 1938) [*Guembelina*]
Heterohelix rajagopalani (Govindan, 1970) [*Gublerina*]
Heterohelix semicostata (Cushman, 1938) [*Guembelina*]
Laeviheterohelix cf. *dentata* (Stenestad, 1968) [*Heterohelix*]
Laeviheterohelix glabrans (Cushman, 1938) [*Guembelina*]
Planoglobulina acervulinoides (Egger, 1899) [*Guembelina*]

- Planoglobulina* cf. *carseyae* (Plummer, 1931) [*Ventilabrella*]
Planoglobulina multicamerata (De Klasz, 1953) [*Ventilabrella*]
Planoglobulina riograndensis (Martin, 1972) [*Ventilabrella*]
Pseudoguembelina costulata (Cushman, 1938) [*Guembelina*]
Pseudoguembelina excolata (Cushman, 1926) [*Guembelina*]
Pseudoguembelina palpebra Brönnimann & Brown 1953
Pseudotextularia cushmani Brown, 1969
Pseudotextularia elegans (Rzehak, 1891) [*Cuneolina*]
Pseudotextularia intermedia de Klasz 1953
Racemiguembelina fructicosa (Egger, 1899) [*Gümbelina*]
Racemiguembelina powelli Smith & Pessagno, 1973
Rugoglobigerina hexacamerata Brönnimann, 1952
Rugoglobigerina milamensis Smith & Pessagno, 1973
Rugoglobigerina pennyi Brönnimann, 1952 [*Rugoglobigerina rugosa* subsp.]
Rugoglobigerina rotundata Brönnimann, 1952 [*Rugoglobigerina rugosa* subsp.]
Rugoglobigerina rugosa (Plummer, 1926) [*Globigerina*]
Rugotruncana subcircumnodifer (Gandolfi, 1955) [*Globotruncana circumnodifer* subsp.]

Selected benthonic foraminifera

- Bolivinoidea australis* Edgell, 1954 [*Bolivinoidea decorata* subsp.]
Bolivinoidea delicatulus Cushman, 1927 [*Bolivinoidea decorata* subsp.]
Bolivinoidea draco (Marsson, 1878) [*Bolivina*]
Bolivinoidea giganteus Hiltermann & Koch, 1950 [*Bolivinoidea decorata* subsp.]
Bolivinoidea miliaris Hiltermann & Koch, 1950 [*Bolivinoidea draco* subsp.]
Stensioeina pommerana Brotzen, 1936

Manuscript received 14 August 2001

Manuscript accepted 25 January 2003

REFERENCES

- AGSO North West Shelf Study Group 1994. Deep reflections on the North West Shelf: changing perceptions of basin formation. In: Purcell, P.G. & Purcell, R.R. (Eds), *The Sedimentary Basins of Western Australia: Proceedings of the Petroleum Exploration Society of Australia Symposium*: 63–76.
- Apthorpe, M.C. 1979. Depositional history of the Upper Cretaceous of the Northwest Shelf, based upon Foraminifera. *The APPEA Journal*, **19**: 74–89.
- Audley-Charles, M.G. 1988. Evolution of the southern margin of Tethys (North Australian region) from early Permian to late Cretaceous. In: Audley-Charles, M.G. & Hallam, A. (Eds), *Gondwana and Tethys*. Geological Society, London, Special Publications, **37**: 79–100.
- Audley-Charles, M.G., Ballantine, P.D. & Hall, R. 1988. Mesozoic–Cenozoic rift–drift sequence of Asian fragments from Gondwanaland. *Tectonophysics*, **155**: 317–330.
- Baillie, P.W., Powell, C.M., Li, Z.X. & Ryall, A.M. 1994. The tectonic framework of Western Australia's Neoproterozoic to Recent sedimentary basins. In: Purcell, P.G. & Purcell, R.R. (Eds), *The Sedimentary Basins of Western Australia: Proceedings of the Petroleum Exploration Society of Australia Symposium*: 45–62.
- Barrera, E. 1994. Global environmental changes preceding the Cretaceous–Tertiary boundary: Early–late Maastrichtian transition. *Geology*, **22**: 877–880.
- Barrera, E., Savin, S.M., Thomas, E. & Jones, C.E. 1997. Evidence for thermohaline-circulation reversals controlled by sea-level change in the latest Cretaceous. *Geology*, **25**: 715–718.

- Bergen, J.A. & Sikora, P.J. 1999. Microfossil diachronism in southern Norwegian North Sea chalks: Valhall and Hod fields. In: Jones, R.W. & Simmons, M.D. (Eds), *Biostratigraphy in Production and Development Geology*. Geological Society, London, Special Publications, **152**: 85–111.
- Boersma, A. 1981. Cretaceous and Tertiary foraminifera from Deep Sea Drilling Project leg 62 sites in the Central Pacific. In: Thiede, J. & Vallier, T.L. (Eds), *Initial Reports of the Deep Sea Drilling Project*, U.S. Government. Washington D.C., 377–396.
- Bown, P.R. 1998. *Calcareous Nannofossil Biostratigraphy*. British Micropalaeontology Society Publications Series, Chapman & Hall/Kluwer Academic Press, 314 pp.
- Bown, P.R. & Young, J.R. 1998. Techniques. In: Bown, P.R. (Ed.), *Calcareous Nannofossil Biostratigraphy*. British Micropalaeontology Society Publications Series, Chapman & Hall/Kluwer Academic Press, 16–28.
- Bralower, T.J. & Bergen, J.A. 1998. Cenomanian–Santonian calcareous nannofossil biostratigraphy of a transect of cores drilled across the Western Interior Seaway. In: Dean, W.E. & Arthur, M.A. (Eds), *Stratigraphy and paleoenvironments of the Cretaceous Western Interior Seaway, USA*. SEPM concepts in sedimentology and paleontology, **6**: 59–77.
- Bralower, T.J. & Siesser, W.G. 1992. Cretaceous calcareous nannofossil biostratigraphy of sites 761, 762, and 763 Exmouth and Wombat plateaus, Northwest Australia. *Proceedings of the Ocean Drilling Program, Scientific Results*, **122**: 601–632.
- Bukry, D. 1969. Upper Cretaceous coccoliths from Texas and Europe. *The University of Kansas Paleontological Contributions*, **51** (Protista 2: 1–79).
- Burnett, J.A. 1997a. New species and biostratigraphical application of *Ceratolithoides* Bramlette and Martini, 1964 from the Campanian and Maastrichtian of the Indian Ocean. *Journal of Nanoplankton Research*, **19**: 123–131.
- Burnett, J.A. 1997b. New species and new combinations of Cretaceous nannofossils, and a note on the origin of *Petrarhabdus* (Deflandre) Wind & Wise. *Journal of Nanoplankton Research*, **19**: 133–142.
- Burnett, J.A. 1998. Upper Cretaceous. In: Bown, P.R. (Ed.), *Calcareous Nannofossil Biostratigraphy*. British Micropalaeontology Society Publications Series, Chapman & Hall/Kluwer Academic Press, 132–199.
- Burnett, J.A., Hancock, J.M., Kennedy, W.J. & Lord, A.R. 1992. Macrofossil, planktonic foraminiferal and nannofossil zonation at the Campanian/Maastrichtian boundary. *Newsletters on Stratigraphy*, **27**: 157–172.
- Burnett, J.A., Kennedy, W.J. & Ward, P. 1992. Maastrichtian nannofossil biostratigraphy in the Biscay region (south-western France, northern Spain). *Newsletters on Stratigraphy*, **26**: 145–155.
- Caron, M. 1985. Cretaceous planktic foraminifera. In: Bolli, H.M., Saunders, J.B. & Perch-Nielsen, K. (Eds), *Plankton Stratigraphy*, **1**: 17–86.
- Chungkham, P. & Jafar, S.A. 1998. Late Cretaceous (Santonian–Maastrichtian) integrated coccolith–globotruncanid biostratigraphy of pelagic limestones from the accretionary prism of Manipur, north-eastern India. *Micropaleontology*, **44**: 69–83.
- Clarke, L.J. & Jenkyns, H.C. 1999. New oxygen isotope evidence for long-term Cretaceous climatic change in the Southern Hemisphere. *Geology*, **27**: 699–702.
- Dalbiez, F. 1955. The genus *Globotruncana* in Tunisia. *Micropaleontology*, **1**: 161–171.
- Ellis, B.F. & Messina, A.R. 1945 et seq. *Catalogue of Foraminifera*. Special Publication, American Museum of Natural History.
- Exon, N.P., Haq, B.U. & von Rad, U. 1992. Exmouth Plateau revisited: scientific drilling and geological framework. *Proceedings of the Ocean Drilling Program, Scientific Results*, **122**: 3–22.
- Exon, N.F., Borella, P.E. & Ito, M. 1992. Sedimentology of marine Cretaceous sequences in the central Exmouth Plateau (northwest Australia). *Proceedings of the Ocean Drilling Program, Scientific Results*, **122**: 233–258.
- Frank, T.D. & Arthur, M.A. 1999. Tectonic forcings of Maastrichtian ocean-climate evolution. *Palaeoceanography*, **14**: 103–117.
- Gardin, S. & Monechi, S. 2001. Calcareous nannofossil distribution in the Tercis geological site (Landes, SW France) around the Campanian–Maastrichtian boundary. In: Odin, G.S. (Ed.), *The Campanian–Maastrichtian Boundary*. Developments in Palaeontology and Stratigraphy, **19**, Elsevier. Amsterdam, 272–292.
- Gardin, S., Odin, G.S., Bonnemaïson, M., Melinte, M., Monechi, S. & von Salis, K. 2001. Results of the cooperative study on the calcareous nannofossils across the Campanian–Maastrichtian boundary at Tercis les Bains (Landes, France). In: Odin, G.S. (Ed.), *The Campanian–Maastrichtian Boundary*. IUGS Special Publication (monograph) Series 36, Developments in Palaeontology and Stratigraphy, **19**, Elsevier. Amsterdam, 293–309.
- Glaessner, M.F. 1948. *Principles of Micropaleontology*, John Wiley and Sons. New York, 296 pp.
- Golovchenko, X., Borella, P.E. & O'Connell, S. 1992. Sedimentary cycles on the Exmouth Plateau. *Proceedings of the Ocean Drilling Program, Scientific Results*, **122**: 279–291.
- Gradstein, F.M., Agterberg, F.P., Ogg, J.G., Hardenbol, J., van Veen, P., Thierry, J. & Huang, Z. 1994. A Mesozoic time scale. *Journal of Geophysical Research*, **99**: 24051–24074.
- Haq, B.U., Hardenbol, J. & Vail, P.R. 1987. Chronology of fluctuating sea levels since the Triassic. *Science*, **235**: 1156–1166.
- Haq, B.U., von Rad, U. & 26 others 1990. Site 761. *Proceedings of the Ocean Drilling Program, Initial Reports*, **12**: 161–211.
- Haq, B.U., von Rad, U. & 26 others 1990. Site 762. *Proceedings of the Ocean Drilling Program, Initial Reports*, **122**: 213–288.
- Hardenbol, J. & Robaszynski, F. 1998. Introduction to the Upper Cretaceous. In: de Graciansky, P.C., Hardenbol, J., Jacquin, T., Vail, P.R. & Farley, M.B. (Eds), *Mesozoic and Cenozoic Sequence Stratigraphy of European Basins*. Society of Economic Paleontologists and Mineralogists, Special Publication, **60**: 329–332.
- Henricksson, A.S. 1993. Biochronology of the terminal Cretaceous calcareous nannofossil Zone of *Micula prinsii*. *Cretaceous Research*, **14**: 59–68.
- Holmes, M.A. & Watkins, D.K. 1992. Middle and Late Cretaceous history of the Indian Ocean. *Synthesis of Results from Scientific Drilling in the Indian Ocean, Geophysical Monograph*, **70**: 225–244.
- Hornibrook, N.d.B., Brazier, R.C. & Strong, C.P. 1989. Manual of New Zealand Permian to Pleistocene Foraminiferal Biostratigraphy. *New Zealand Geological Paleontological Bulletin*, **56**: 175 pp.
- Howe, R.W., Haig, D.W. & Aphorpe, M.C. 2000. Cenomanian–Coniacian transition from siliciclastic to carbonate marine deposition, Giralia Anticline, Southern Carnarvon Platform, Western Australia. *Cretaceous Research*, **21**: 517–551.
- Huang, Z., Boyd, R. & O'Connell, S. 1992. Upper Cretaceous cyclic sediments from Hole 762C, Exmouth Plateau, northwest Australia. *Proceedings of the Ocean Drilling Program, Scientific Results*, **122**: 259–277.
- Huber, B.T. 1990. Maastrichtian planktonic foraminifer biostratigraphy of the Maud Rise (Weddell Sea, Antarctica): ODP Leg 113 Holes 689B and 690C. *Proceedings of the Ocean Drilling Program, Scientific Results*, **113**: 489–513.
- Huber, B.T. 1991. Maastrichtian planktonic foraminifer biostratigraphy and the Cretaceous/Tertiary boundary at Hole 738C (Kerguelen Plateau, Southern Indian Ocean). *Proceedings of the Ocean Drilling Program, Scientific Results*, **114**: 451–495.
- Huber, B.T. 1992. Paleobiogeography of Campanian–Maastrichtian foraminifera in the southern high latitudes. *Palaeogeography, Palaeoclimatology, Palaeoecology*, **92**: 325–360.
- Huber, B.T., Hodell, D.A. & Hamilton, C.P. 1995. Middle–Late Cretaceous climate of the southern high latitudes: Stable isotopic evidence for minimal equator–pole thermal gradients. *Geological Survey of America Bulletin*, **107**: 1164–1191.
- Ion, J. & Odin, G.S. 2001. Preliminary study of the benthic foraminifera of the Campanian–Maastrichtian section at Tercis les Bains (Landes, France). In: Odin, G.S. (Ed.), *The Campanian–Maastrichtian Boundary*. IUGS Special Publication (monograph) Series 36, Developments in Palaeontology and Stratigraphy, **19**, Elsevier. Amsterdam, 310–327.
- Kennedy, W.J., Cobban, W.A. & Scott, G.R. 1992. Ammonite correlation of the uppermost Campanian of Western Europe, the U.S. Gulf Coast, Atlantic Seaboard and Western Interior, and the numerical age of the base of the Maastrichtian. *Geological Magazine*, **129**: 497–500.

- Kennard, J.M., Deighton, I., Edwards, D.S., Colwell, J.B., O'Brien, G.W. & Boreham, C.J. 1999. Thermal history modelling and transient heat pulses: new insights into hydrocarbon expulsion and 'hot flushes' in the Vulcan Sub-basin, Timor Sea. *The APPEA Journal*, **39**: 177–207.
- Kucera, M. & Malmgren, B.A. 1996. Latitudinal variation in the planktic foraminifer *Contusotruncana contusa* in the terminal Cretaceous ocean. *Marine Micropaleontology*, **28**: 31–52.
- MacLeod, K.G. 1994. Extinction of Inoceramid bivalves in Maastrichtian strata of the Bay of Biscay region of France and Spain. *Journal of Paleontology*, **68**: 1048–1066.
- MacLeod, K.G. 1994. Bioturbation, inoceramid extinction, and mid-Maastrichtian ecological change. *Geology*, **22**: 139–142.
- MacLeod, K.G. & Huber, B.T. 1996. Reorganization of deep ocean circulation accompanying a Late Cretaceous extinction event. *Nature*, **380**: 422–425.
- McNamara, K.J., Rexilius, J.P., Marshall, N.G. & Henderson, R.A. 1988. The first record of a Maastrichtian ammonite from the Perth Basin, Western Australia, and its biostratigraphical significance. *Alcheringa*, **12**: 163–168.
- Melinte, M. & Odin, G.S. 2001. Optical study of the calcareous nannofossils from Tercis les Bains (Landes, France) across the Campanian–Maastrichtian boundary. In: Odin, G.S. (Ed.), *The Campanian–Maastrichtian Boundary*. IUGS Special Publication (monograph) Series 36, Developments in Palaeontology and Stratigraphy, **19**. Elsevier, Amsterdam, 285–292.
- Metcalf, I. 1996. Gondwanaland dispersion, Asian accretion and evolution of eastern Tethys. *Australian Journal of Earth Sciences*, **43**: 605–623.
- Mory, A.J. 1988. Regional geology of the offshore Bonaparte Basin. In: Purcell, P.G. & Purcell, R.R. (Eds), *The North West Shelf, Australia: Proceedings of Petroleum Exploration Society Australia Symposium*, Perth, 287–310.
- Müller, R.D., Mihut, D. & Baldwin, S. 1998. A new kinematic model for the formation and evolution of the west and northwest Australian Margin. In: Purcell, P.G. & Purcell, R.R. (Eds), *The Sedimentary Basins of Western Australia 2: Proceedings of Petroleum Exploration Society Australia Symposium*, Perth, 73–80.
- Nederbragt, A.J. 1991. Late Cretaceous biostratigraphy and development of Heterohelidae (planktic foraminifera). *Micropaleontology*, **37**: 329–372.
- Nederbragt, A.J. 1998. Quantitative biogeography of late Maastrichtian planktic foraminifera. *Micropaleontology*, **44**: 385–412.
- Nöel, D. 1956. Cocolithes des terrains Jurassiques de l'Algérie. *Publications, Service de la Carte Géologique (Algérie), Bulletin*, **8**: 303–345.
- O'Brien, G.W., Etheridge, M.A., Willcox, J.B., Morse, M., Symonds, P., Norman, C. & Needham, D.J. 1993. The structural architecture of the Timor Sea, North-Western Australia: implications for basin development and hydrocarbon exploration. *The APPEA Journal*, **33**: 258–277.
- O'Brien, G.W., Morse, M., Wilson, D., Quiafe, P., Colwell, J., Higgins, R. & Foster, C.B. 1999. Margin-scale, basement-involved compartmentalisation of Australia's North West Shelf: a primary control on basin-scale rift, depositional and reactivation histories. *The APPEA Journal*, **39**: 40–63.
- Odin, G.S. 1996. Definition of a Global Boundary Stratotype Section and Point for the Campanian/Maastrichtian boundary. In: Rawson, P.F. (Ed.), *Second International Symposium on Cretaceous Stage Boundaries, Brussels, Sciences de la Terre Aardwetenschappen, Bulletin de l'Institut royal des Sciences naturelles de Belgique*, **66-Supp**: 111–117.
- Odin, G.S. 2001a. *The Campanian–Maastrichtian Stage Boundary*. IUGS Special Publication (monograph) Series 36, Developments in Palaeontology and Stratigraphy, **19**. Elsevier, Amsterdam, 881 pp.
- Odin, G.S. 2001b. Numerical age calibration of the Campanian–Maastrichtian succession at Tercis les Bains (Landes, France) and in the Bottaccione Gorge (Italy). In: Odin, G.S. (Ed.), *The Campanian–Maastrichtian Boundary*. IUGS Special Publication (monograph) Series 36, Developments in Palaeontology and Stratigraphy, **19**. Elsevier, Amsterdam, 775–782.
- Odin, G.S., Arz, J.A., Caron, M. & Ion, J. 2001. *et al.* Campanian–Maastrichtian planktonic foraminifera at Tercis les Bains (Landes, France); synthetic view and potential for global correlation. In: Odin, G.S. (Ed.), *The Campanian–Maastrichtian Boundary*. IUGS Special Publication (monograph) Series 36, Developments in Palaeontology and Stratigraphy, **19**. Elsevier, Amsterdam, 379–395.
- Pattillo, J. & Nicholls, P.J. 1990. A tectonostratigraphic framework for the Vulcan Graben, Timor Sea region. *The APEA Journal*, **30**: 27–51.
- Perch-Nielsen, K. 1985. Mesozoic calcareous nannofossils. In: Bolli, H.M., Saunders, J.B. & Perch-Nielsen, K. (Eds), *Plankton Stratigraphy*. Cambridge University Press, Cambridge, 329–426.
- Pessagno, E.A. 1967. Upper Cretaceous planktonic foraminifera from the western Gulf Coastal Plain. *Palaeontographica America*, **5**: 245–445.
- Petrizzo, M.R. 2000. Upper Turonian–lower Campanian planktonic foraminifera from southern mid-high latitudes (Exmouth Plateau, NW Australia): biostratigraphy and taxonomic notes. *Cretaceous Research*, **21**: 479–505.
- Pospichal, J.J. & Bralower, T.J. 1992. Calcareous nannofossils across the Cretaceous/Tertiary boundary, Site 761, northwest Australian margin. *Proceedings of the Ocean Drilling Program, Scientific Results*, **122**: 735–752.
- Powell, C.M., Roots, S.R. & Veevers, J.J. 1988. Pre-breakup continental extension in East Gondwanaland and the early opening of the eastern Indian Ocean. *Tectonophysics*, **155**: 261–283.
- Premoli-Silva, I. & Sliter, W.V. 1994. Cretaceous planktonic foraminiferal biostratigraphy and evolutionary trends from the Bottaccione section, Gubbio, Italy. *Palaeontographia Italica*, **82**: 1–89.
- Premoli-Silva, I. & Sliter, W.V. 1999. Cretaceous paleoceanography: Evidence from planktonic foraminiferal evolution. In: Barrera, E. & Johnson, C.C. (Eds), *Evolution of the Cretaceous ocean-climate system*. Geological Society of America, Boulder, Special Paper, **332**: 301–328.
- Rexilius, J.P. 1984. *Late Cretaceous foraminiferal and calcareous nannoplankton biostratigraphy, Southwestern Australian Margin*. PhD Thesis. Department of Geology & Geophysics, The University of Western Australia, Perth, Western Australia, 291 pp.
- Risatti, J.B. 1973. Nannoplankton biostratigraphy of the upper Bluffport Marl-lower Prairie Bluff Chalk interval (upper Cretaceous), in Mississippi. In: Smith, L.A. & Hardenbol, J. (Eds), *Proceedings of a symposium on calcareous nannofossils*. Society of Economic Paleontologists and Mineralogists, Gulf Coast Section, Houston, Texas, 8–57.
- Robaszynski, F., Caron, M., Donoso, J.M.G. & Wonders, A.A.H. *et al.* 1984. Atlas of late Cretaceous Globotruncanids. *Revue de Micropaleontologie*, **26**: 145–305.
- Robaszynski, F. & Caron, M. 1995. Foraminifères planctoniques du Cretace: commentaire de la zonation Europe-Mediterranee. *Bulletin de la Société Géologique de France*, **166**: 681–692.
- Roth, P.H. 1978. Cretaceous nannoplankton biostratigraphy and oceanography of the Northwestern Atlantic Ocean. *Initial Reports of the Deep Sea Drilling Project*, **44**: 731–760.
- Scotese, C.R., Gahagan, L.M. & Larson, R.L. 1988. Plate tectonic reconstruction of the Cretaceous and Cenozoic ocean basins. *Tectonophysics*, **155**: 27–48.
- Shafik, S. 1990. Late Cretaceous nannofossil biostratigraphy and biogeography of the Australian western margin. *Australian Bureau of Mineral Resources, Report*, **295**: 164 pp.
- Shafik, S. 1993. Albian and Maastrichtian nannofloral biogeographic provinces in Western Australia. *Australian Geological Survey Organisation Research Newsletter*, **19**: 15.
- Shafik, S. 1998. Problems with the Cretaceous biostratigraphic system of Australia: time for a review. *Australian Geological Survey Organisation Research Newsletter*, **28**: 12–14.
- Sigal, J. 1977. Essai de zonation du Cretace mediterraneen a l'aide des foraminifères planctoniques. *Geologie Méditerranéenne*, **4**: 99–108.
- Sissingh, W. 1977. Biostratigraphy of Cretaceous calcareous nannoplankton. *Geologie en Mijnbouw*, **56**: 37–65.
- Smith, C.C. & Pessagno, E.A. 1973. Planktonic foraminifera and stratigraphy of the Corsicana Formation (Maestrichtian) north-

- central Texas. *Cushman Foundation for Foraminiferal Research, Special Publication*, **12**: 68 pp.
- Struckmeyer, H.I.M., Yeung, M. & Bradshaw, M.T. 1990. Mesozoic palaeogeography of the northern margin of the Australian Plate and its implications for hydrocarbon exploration. In: Carman, G.J. & Carman, Z. (Eds), *Petroleum Exploration in Papua New Guinea: Proceedings of the First PNG Petroleum Convention*: 137–152.
- Thierstein, H.R. 1981. Late Cretaceous nannoplankton and the change at the Cretaceous–Tertiary boundary. In: Warme, J.E., Douglas, R.G. & Winterer, E.L. (Eds), *The Deep Sea Drilling Project: a decade of progress*. SEPM Special Publication: 355–394.
- Tronchetti, G. 2001. Les foraminifères benthiques des affleurements campano-maastrichtiens de Tercis les Bains (Landes, France). In: Odin, G.S. (Ed.), *The Campanian–Maastrichtian Boundary*. Developments in Palaeontology and Stratigraphy, **19**, Elsevier. Amsterdam, 314–327.
- Tronchetti, G., Ion, J. & Odin, G.S. 2001. Benthic foraminifera of the Campanian–Maastrichtian geological site at Tercis les Bains (France); synthesis. In: Odin, G.S. (Ed.), *Developments in Palaeontology and Stratigraphy*, **19**, Elsevier. Amsterdam, 328–337.
- van Hinte, J.E. 1976. A Cretaceous time scale. *Bulletin of the American Association of Petroleum Geologists*, **60**: 498–516.
- von Salis, K. 2001. Calcareous nannofossils around the Campanian/Maastrichtian Boundary at Tercis, France. In: Odin, G.S. (Ed.), *The Campanian–Maastrichtian Boundary*. Developments in Palaeontology and Stratigraphy, **19**, Elsevier. Amsterdam, 268–271.
- Veevers, J.J. & Powell, C.M. 1990. Phanerozoic tectonic regimes of Australia reflect global events. *Journal of Structural Geology*, **12**: 545–551.
- Veevers, J.J., Powell, C.M. & Roots, S.R. 1991. Review of seafloor spreading around Australia. I. Synthesis of the patterns of spreading. *Australian Journal of Earth Sciences*, **38**: 373–389.
- von Rad, U. & Bralower, T.J. 1992. Unique record of an incipient ocean basin: Lower Cretaceous sediments from the southern margin of Tethys. *Geology*, **20**: 551–555.
- von Rad, U., Exon, N.F. & Haq, B.U. 1992. Rift-to-drift history of the Wombat Plateau, northwest Australia: Triassic to Tertiary Leg 122 results. *Proceedings of the Ocean Drilling Program, Scientific Results*, **122**: 765–800.
- Ward, P.D. & Kennedy, W.J. 1993. Maastrichtian ammonites from the Biscay Region (France, Spain). *Journal of Paleontology, Supplement*, **67**: 1–58.
- Watkins, D.K., Wise, S.W. Jr, Pospichal James, J. & Crux, J. 1996. Upper Cretaceous calcareous nannofossil biostratigraphy and paleoceanography of the Southern Ocean. In: Mokuilevsky, A. & Whatley, R. (Eds), *Microfossils and oceanic environments*, University of Wales, Aberystwyth Press, 355–381.
- Webb, P.N. 1973. Upper Cretaceous–Paleocene foraminifera from Site 208 (Lord Howe Rise/Tasman Sea), DSDP, Leg 21. In: Burns, R.E. & Andrews, J.E. (Eds), *Initial Reports of the Deep Sea Drilling Project, Leg 21*, US Government Printing Office. Washington D.C., 541–573.
- Wonders, A.A.H. 1980. Middle and Late Cretaceous planktonic Foraminifera of the Western Mediterranean area. *Utrecht Micropaleontology Bulletin*, **24**: 1–158.
- Wonders, A.A.H. 1992. Cretaceous planktonic foraminiferal biostratigraphy, Leg 122, Exmouth Plateau, Australia. *Proceedings of the Ocean Drilling Program, Scientific Results*, **122**: 587–599.
- Wright, C.A. & Apthorpe, M. 1976. Planktonic foraminiferids from the Maastrichtian of the Northwest Shelf, Western Australia. *Journal of Foraminiferal Research*, **6**: 228–241.
- Wright, C.A. & Apthorpe, M. 1995. C.A. Wright's Cretaceous planktonic foraminiferal zonation for the Northwest Shelf, Australia. (abstract) *Second International Symposium on Cretaceous Stage Boundaries*, Institut Royal des Sciences Naturelles de Belgique. Brussels, 128.
- Young, J.R., Bergen, J.A. & Bown, P.R. et al. 1997. Guidelines for coccolith and calcareous nannofossil terminology. *Palaeontology*, **40**(4): 875–912.
- Zepeda, M.A. 1998. Planktonic foraminiferal diversity, equitability and biostratigraphy of the uppermost Campanian – Maastrichtian, ODP Leg 122, Hole 762C, Exmouth Plateau, NW Australia, eastern Indian Ocean. *Cretaceous Research*, **19**: 117–152.